

**CONSTRUCTION, EXPRESSION, AND PURIFICATION OF  
SOLUBLE CD16 IN BACTERIA**

A Thesis  
Presented to  
The Academic Faculty

By

Christopher Sinotte

In Partial Fulfillment  
of the Requirements for the Degree  
Masters of Science in Bioengineering

Georgia Institute of Technology

8/2006

**CONSTRUCTION, EXPRESSION, AND PURIFICATION OF  
SOLUBLE CD16 IN BACTERIA**

Approved by:

Dr. Cheng Zhu, Advisor  
Schools of Mechanical Engineering  
*Georgia Institute of Technology*

Dr. Allen Orville  
School of Chemistry and Biochemistry  
*Georgia Institute of Technology*

Dr. Periasamy Selvaraj  
School of Medicine  
*Emory University*

Dr. Robert Butera  
School of Electrical and Computer  
Engineering  
*Georgia Institute of Technology*

Date Approved: May 11, 2006

## ACKNOWLEDGEMENTS

I would like to thank Dr. Cheng Zhu for giving me the opportunity to conduct meaningful research and furthering my education. The environment and guidance that you provided is of the highest quality. You are a great leader and teacher. I have learned much from you.

I would like to thank Dr. Periasamy Selvaraj for giving me day to day guidance in my experiments and for welcoming me into his lab. You provided me a wonderful experience that I will never forget. Your lab is one of a kind and I have grown close to each of your researchers.

I would like to thank my fellow researchers in each of my labs. I would especially like to thank Murthy and Nimita as your friendship and assistance have been incredible. You have taught me much and your ideas have helped me on many occasions.

Finally, I would like to thank my parents, Bob and Nancy, as well as Katie, Andy, Nomar, and Trot. Your endless support and love through the years mean the world to me.

# TABLE OF CONTENTS

	Page
ACKNOWLEDGEMENTS	iii
LIST OF TABLES	v
LIST OF FIGURES	vi
LIST OF SYMBOLS	ix
LIST OF ABBREVIATIONS	x
SUMMARY	xi
<u>CHAPTER</u>	
1 Introduction	1
Specific Aims	1
Background and Significance	4
2 Materials and Methods	22
3 Results	33
4 Discussion	47
REFERENCES	56

## LIST OF TABLES

	Page
Table 1: Mutation sites at amino acid 147 and 176 of sCD16 A and B. Letters in bold are the locations for the site specific mutations involved in this project. Mutations cause the underlined letters to change between amino acids D and G at position 147 and between amino acids F and V at position 176.....	33

## LIST OF FIGURES

	Page
Figure 1: Human Fc $\gamma$ R family of receptors [13]. Fc $\gamma$ RIIC, Fc $\gamma$ RIV are not shown. Figure from Fridman, et al., Immunology 2004. Anchorage is accomplished by single pass polypeptide ( $\alpha$ ) or by Glycosyl Phosphatidylinositol (GPI). Associated signaling pathways are depicted by $\gamma$ and $\zeta$ . Fc $\gamma$ RIIa and Fc $\gamma$ RIIb have intrinsic signaling pathways that are incorporated in the $\alpha$ polypeptide anchor. ITAM (activation) and ITIM (inhibitory) are the signaling pathways depicted. ....	6
Figure 2: Solved crystal structures of Fc $\epsilon$ RI $\alpha$ , 2A, (MMDB #13689, PDB #1F2Q) [28], and of the Fc $\epsilon$ RI $\alpha$ - IgE-Fc complex, 2B, (MMDB # 13872, PDB #1F6A) [33], from Entrez Molecular Modeling Database (MMDB) [71].....	11
Figure 3: Side view of Fc $\epsilon$ RI $\alpha$ in ribbon form, 3A. Binding residues are in stick form while strands are labeled [33]. Superposition of Fc $\epsilon$ RI $\alpha$ -IgE-Fc complex (beige) with Fc $\gamma$ RIIB-IgG-Fc complex (green), 3B. Arrows indicate domains used to superimpose complexes [33]. Figure from Garman, et al. (MMDB #14309, PDB #1FP5) [33].....	11
Figure 4: Fc $\gamma$ RIIA structure, 4A, in ribbon form. Strands are lettered A-G while D1 domain is blue and D2 domain is green with an angle of 52° between them. Ribbon diagram of an Fc $\gamma$ RIIA dimer, 4B. Figure from Maxwell, et al. (MMDB #13259, PDB #1FCG) [29].....	13
Figure 5: Structure of human sFc $\gamma$ RIIB in ribbon form. Red loops are interaction sites for IgG binding. Ball and stick formations are key residues for IgG binding and the disulfide bridge. Green Balls are potential N-glycosylation sites. Figure from Sondermann, et al. (MMDB #12664, PDB #2FCB) [30].....	14
Figure 6: Structure of sCD16B in two forms. sCD16B, 6A, (MMDB #14218, PDB #1E4J) [4, 71]. Stereo ribbon structure of sCD16B, 6B, with IgG contact residues in ball and stick formation. Green contacts C $\gamma$ 2-B while magenta contacts C $\gamma$ 2-A. Large balls (blue) are potential glycosylation sites and disulfide bridge is yellow. Figure B from Sondermann, et al. [18].....	15
Figure 7: The structure of the sFc $\gamma$ RIII-hFc1 complex in the vertical view, a, and in the 90° rotated side view, b. Ball and stick figures represent the “proline sandwich” while larger blue spheres exhibit glycosylation sites [4]. Figures created by MOLSCRIPT [72]. Figure from Sondermann, et al.(MMDB #14214, PDB #1E4K) [4].....	16

- Figure 8: Structure of FcγRIII [5] created by MOLSCRIPT [72]. A, FcγRIII's (ribbon form) binding loops are red, D1 domain is blue, D2 domain is green. B, KIR's domain orientation (ribbon form) resembling FcγRIII. C, FcγRIII's (ribbon form) interdomain region focusing on the packing domains (dark blue and green). Residues and domains are labeled in the figure. D, Asymmetric unit containing superimposed molecules A and B of FcγRIII. Figure from Zhang, et al. (MMDB #14531, PDB #1FNL) [5]..... 18
- Figure 9: FcR structures superimposed [18]. Disulphide bridges in yellow. The color of the FcR name is the color of the structure. Figure from Sondermann, et al. (PDB #'s 1FCG, 2FCB, 1FNL, 1EFJ, 1F6A) [18]..... 18
- Figure 10: Sequence alignment of the FcR family [4] created by ALSCRIPT [73]. Magenta depicts conserved cysteines. Potential glycosylation sites are in blue. Orange depicts identical residues in the first domain, while those identical in the second domain are pink and those identical in both are green. Contact between domains by way of residue side chains are depicted in red arrows, while blue arrows are binding contact to IgG. Figure from Sondermann, et al. [4]..... 21
- Figure 11: Construction of soluble CD16 gene and insertion into the pET 21a+ vector. 24
- Figure 12: Cartoon depicting the locations of the amino acid mutations at position 147 and 176 in both CD16A and CD16B..... 34
- Figure 13: Western Blot analysis on sCD16 induction pathways results after SDS-PAGE. Monoclonal 214.1 was the primary antibody. Lane 1 is sCD16A expressed in the BL21-AI pathway (Invitrogen). Lane 2 is sCD16A expressed in the BL21 RIPL pathway (Stratagene). Lane 3 contains CD16A-Ig complex. Bio-Rad 12% Tris polyacrylamide gel and Bio-Rad nitrocellulose membrane were used..... 35
- Figure 14: A, Western Blot analysis of SDS-PAGE. Lane 1 contains CD16A-Ig. Lanes 2, 3, 4, and 5 contain sCD16A expressed in the BL21-AI pathway for 4, 5, 6, and 8 hours, respectively. Protein expressed at an OD 600 nm value of 0.4 using 0.2% Arabinose and 1 mM IPTG. B, The expression pathway of BL21-AI (Invitrogen) [49]..... 36
- Figure 15: A, sCD16B<sup>NA2</sup> V176F inclusion bodies induced in BL21-AI pathway under different conditions. Lanes 1-3 are induced at 1.0 OD 600 nm, while 4-6 are induced at 1.5. Lanes 1 and 4, 2 and 5, and 3 and 6 were induced for 8, 10, and 12 hours, respectively. B, sCD16BNA2 D147G induced for 10 hours in the BL21-AI pathway at 1.0 OD 600 nm with .2% L-Arabinose and 1 mM IPTG. Lane 1 contains the inclusion bodies, while 2-5 contain sonication supernatants..... 37

- Figure 16: A, inclusion bodies expressed at 1.0 OD 600nm for 8 hours after inducing with 0.2% Arabinose and 1 mM IPTG in the BL21-AI pathway. Sonication steps included 90 second intervals of sonic treatment. Lane 2 is wild type sCD16A and Lane 3 is the sCD16A F176V mutant. B, sCD16A G147D mutant expressed with the same conditions as part A. Lane 1 is sCD16A G147D inclusion bodies, while Lanes 2 through 5 are the sonication supernatants in order. C, An example of a poor inclusion bodies sample. Lane 1 is the poor inclusion body sample and Lanes 2 through 7 are the sonication supernatants. All three gels were 12% Tris-Hcl (Bio-Rad) with 50  $\mu$ l wells. All samples were 25  $\mu$ l inclusion bodies and 25  $\mu$ l reducing buffer..... 39
- Figure 17: SDS-PAGE of refolded sCD16A wild type fractions from G-200 Sephadex size exclusion column with a Urea gradient. Proteins were not separated well enough and are far too low in concentration to make a final refolded sCD16 solution of 10 mg/ml. A Bio-Rad 12% Tris-HCl polyacrylamide gel was used with 25 $\mu$ l sample..... 41
- Figure 18:A, SDS-PAGE analysis on refolded sCD16 proteins. Lane 1 is refolded wild type sCD16A protein and Lane 2 is refolded sCD16A F176V mutant protein. Both samples taken from the post stir cell concentration solution. Lanes 3 and 4 are the same wild type and mutant protein after a second concentration in Pierce iCON concentrators. B, The same process as A, only with refolded sCD16A G147D mutant..... 43
- Figure 19:SDS-PAGE of S-300 fraction contained sCD16A wild type..... 45
- Figure 20: Results of Sandwich ELISA. See text for explanation of experiment. CD16A-Ig was used as a positive control, while BSA solution served as a negative control..... 46
- Figure 21:Rosetting assay for CD16 Mutants. Rosetting results (Figure 19) show binding activity of wild type CD16A and the six site specific CD16 mutants expressed in a eukaryotic pathway. Experiment performed by Ravichandran Panchanathan..... 49
- Figure 22:Rosetting results for Figure 18. A, Results show expression of CD16 mutants on CHO-K1 cells. B, Results show CD16A does not bind to monomeric IgG..... 50
- Figure 23: SDS-PAGE washing results of refolded wild type sCD16A. A, One washing step with 10 mM Tris buffer to help rid solution of unwanted protein. Lanes 1 and 3 are the same (pre-washing), as are Lanes 2 and 4 (post washing). Lanes 3 and 4 are is the negative representation to aid in viewing the bands. B, A second example of washing to rid solution of trace proteins..... 54

## LIST OF SYMBOLS

$\gamma$	gamma
$\text{\AA}$	angstrom
$^\circ$	degree
$\alpha$	alpha
$\varepsilon$	epsilon
$\Delta$	delta

## LIST OF ABBREVIATIONS

CD16	Cluster Designation 16
Fc $\gamma$ RIII	Constant Fragment (Crystallizable) gamma Receptor III for IgG
kD	kiloDalton
IPTG	isopropyl-beta-D-thiogalactopyranoside
PCR	Polymerase Chain Reaction
IgG	Immunoglobulin G
IgE	Immunoglobulin E
mg	milligram
ml	milliliter
GPI	Glycosyl Phosphatidylinositol
Ca <sup>+2</sup>	Calcium
Kd	Dissociate Constant (Receptor affinity)
NA	Neutrophil Antigen
ITAM	Immunoreceptor Tyrosine-based Activation Motif
ITIM	Immunoreceptor Tyrosine-based Inhibitory Motif
ELISA	Enzyme-linked Immunosorbant Assay
CD16B <sup>NA1</sup>	Cluster Designation Subtype B Neutrophil Antigen 1
CD16B <sup>NA2</sup>	Cluster Designation Subtype B Neutrophil Antigen 2
sCD16	soluble (extracellular) Cluster Designation 16
CD64	Cluster Designation 64
CD32	Cluster Designation 32
Fc $\gamma$ R	Constant Fragment (Crystallizable) gamma Receptor

## SUMMARY

CD16 is a physiologically essential Fc $\gamma$  receptor III as either a single-pass transmembrane protein (CD16A) or as a glycosylated phosphatidylinositol (GPI) anchored protein (CD16B) on the surface of immune cells that have been implicated in many autoimmune and immune complex-mediated diseases. Its functions include binding and clearing antibody (IgG) coated foreign pathogens, receptor-mediated phagocytosis, and triggering antibody dependent cellular cytotoxicity. It is well established that these functions depend on protein-protein interaction between CD16 and the Fc domain of IgG. However, the molecular details of CD16-IgG interactions are less well defined, but are essential to developing therapeutic compounds to treat many autoimmune and IC diseases. Stable mammalian cell lines expressing wild-type CD16 isoforms and site-specific mutants, including extracellular soluble fragments of CD16 have been established. Soluble forms of wild type CD16A and these CD16 mutants were expressed in a bacterial pathway in order to amass sufficient quantities for x-ray crystallographic studies.

The soluble portions of wild-type CD16A and several site-specific CD16A and CD16B mutants were constructed by PCR amplification and ligation with a pET vector. The proteins were expressed in a prokaryotic pathway, BL21 AI, for 8-10 hours and lysed to obtain inclusion bodies. A hand-held sonicator was used to wash the inclusion bodies, while a Urea solution separated and dissolved the proteins. The target proteins were then refolded by rapid dilution, concentrated with a stir cell, and purified. Wild type sCD16A and four site specific mutants were constructed with good sequencing, while wild type

sCD16A, sCD16A F176V, and sCD16A G147D were expressed and refolded to optimal levels. X-ray crystallographic data has been collected from sCD16A F176V as a result of these studies and crystals are currently being grown from wild type sCD16A and sCD16A G147D.

# CHAPTER 1

## INTRODUCTION

### Hypothesis

With the prokaryotic expression and crystal growth of wild type soluble CD16A and soluble CD16 site specific mutants, X-ray crystallographic diffraction data can be collected and used to solve various CD16 extracellular structures, lending vital information to ongoing FcγR- IgG complex functional studies and identifying therapeutic schemes in treating autoimmune diseases.

### Specific Aims

Specific Aim 1: *Construction and expression of wild type soluble CD16A along with site-specific mutants.* A prokaryotic expression system will be established to express several forms of soluble CD16 (extracellular portion of FcγRIII). CD16 has two subtypes, A and B, while the B subtype has two polymorphic forms, CD16B<sup>NA1</sup> and CD16B<sup>NA2</sup>. Wild type sCD16A and its site-specific mutants, F176V and G147D, along with the same site-specific mutants for CD16B<sup>NA1</sup> and CD16B<sup>NA2</sup>, will be expressed. The soluble form of membrane receptors is an excellent source for crystallization and subsequent determination of the ternary structure of a receptor. Only the extracellular domain of the CD16 is involved in ligand binding, therefore only this portion of the molecule will be used as it should maintain its functioning ability. The hydrophobic transmembrane domain will be bypassed using PCR.

The CD16 gene from pCDNA 3.1 vectors in *E. coli* bacterial cells (TOP 10 Invitrogen) will be amplified by PCR from Trp-2 to Ser-211. Primer development will create Nde-I and Not-I restriction enzyme sites and a stop codon (amino acid 211). PCR

amplification of the gene takes place, followed by the subsequent digestion (Nde-I and Not-I) and ligation with the new vector, pET 21a+ (Novagen). pET 21a+ includes a C-terminal His-tag sequence and a T7 tag. TOP-10 (Invitrogen) *E. coli* cells will be used for long term storage of the new gene and vector combination. Sequencing on the ligated structure is performed to check the accuracy of the previous steps.

The ligated soluble protein DNA and pET 21a+ vector are transformed into a BL21 expression pathway. Protein is induced with IPTG, both alone and in combination with L-Arabinose depending on the BL21 pathway, for 6-10 hours. The bacterial pellet is to be collected, lysed, and sonicated to obtain treated and washed inclusion bodies.

Specific Aim 2: *Dissolve inclusion bodies, refold sCD16 protein, and obtain high purity.*

Soluble CD16 proteins are found almost exclusively in Inclusion Bodies after lysis [4, 5]. A detergent is used to separate the inclusion bodies and dissolve the proteins. Refolding agents are added and the detergent is removed to force proper folding. Several refolding and concentrating methods are to be tested to find a high enough yield, 10mg/ml concentration of soluble CD16 protein, and a pure enough sample, greater than 90-95% according to SDS-PAGE. Among the refolding techniques are rapid dilution injections, dialysis tubing, and sephadex columns with gradient buffers. Among the concentration methods are stir cells, centrifuge concentrators, polyvinylpyrrolidone powder, and dialysis tubing. And among the purification techniques are washing steps, affinity chromatography, and size exclusion columns. Sandwich ELISA will be used to confirm functional ability.

Specific Aim 3: *Grow crystals and determine the crystal structure of sCD16 protein.*

Previous studies by Sondermann, et al [4], and Zhang, et al [5], established sCD16B crystallization techniques. It is logical to start the sCD16A wild type crystal trials with a similar technique. However, since crystallization techniques are hard to replicate, wide

screening kits should be used in order to cover all crystal solutions. Upon crystal growth, the National Synchrotron Light Source can be used to collect diffraction data. Structure solving by molecular replacement software will be used with CD16B as a template.

## **Background and Significance**

### **1.1 Role of FcγR's In Host Defense**

Cellular receptors for the Fc domain of IgG antibodies, (FcγR), have a crucial role in the development of autoimmune diseases [9, 10, 11, 12]. These receptors link the body's recognition of antigens with cellular responses [14]. FcγR are expressed by immune cells such as neutrophils, monocytes, and dendritic cells, which recognize and eliminate antibody-coated foreign objects. This takes place through FcγR mediated process called ADCC, or antibody-dependent cellular cytotoxicity, and phagocytosis [8]. FcγR can also be occupied by immune complexes, which then induces the secretion of inflammatory mediators and lymphokines [15]. Any error in this process, owing to faulty FcγR function, can cause a number of diseases and disorders.

FcγR has four classes (Figure 1) that belong to the IgG superfamily [13]. There is the high affinity receptor of FcγRI (CD64) which is about 70 kD, expressed on monocytes and tissue macrophages, and has a Kd of  $10^{-8}$  for monomeric IgG [8, 13]. Its high affinity is partially due to its having three related immunoglobulin domains [18]. Next are the low affinity receptors of FcγRII (CD32) and FcγRIII (CD16). Their Kd's for monomeric IgG is between  $10^{-5}$  and  $10^{-7}$  [13] as they have only two related immunoglobulin domains [18]. CD32 has a size of 40 kD [8] and is expressed on B cells, platelets, monocytes, macrophages, neutrophils, epithelial, and endothelial cells [16]. There are three subtypes of CD32: CD32A, CD32B, and CD32C. The A and C subtypes are almost identical, with sequencing showing only a single amino acid difference [17], while subtype B is 93% identical to A [18].

The third FcγR is FcγRIII, or CD16, and is a glycoprotein between 50- 70 kD. It has two subtypes, CD16A and CD16B. CD16A is mainly present on natural killer cells and T cells [13], while CD16B is expressed mainly on neutrophils [8]. Further, CD16B has two polymorphic forms, NA1 and NA2 [19]. The NA stands for neutrophil antigen. These two forms differ slightly in the membrane-distal Ig-like domain, which causes NA1 to bind immune complexed IgG3 more efficiently than NA2 [20]. NA1 also induces phagocytosis of particles opsonized with either IgG1 or IgG3 [19]. CD16A is polypeptide anchored, while CD16B is anchored to the cell surface via a C- terminus GPI moiety [8, 21]. Lastly, CD16 is also found in a soluble form [22, 23] from activated neutrophils that proteolytically cut off the soluble, or extracellular, portion of CD16 that leads to increased production of inflammation mediators. And the fourth class is the recently published FcγRIV, from Ravetch and colleagues [75]. This receptor binds to IgG2a and IgG2b with intermediate affinity and its expression is limited to myeloid lineage cells [75]. Important binding domains in the FcγR-IgG complex will be discussed after Fc receptor structure papers are reviewed.

CD16A and CD16B also hold different signaling methods in the previously mentioned antibody-dependent cellular cytotoxicity [24]. CD16A utilizes an Immunoreceptor Tyrosine-based Activation Motif (ITAM) to aid in the signaling processing of activated natural killer cells, while CD16B, as previously mentioned, has a GPI anchor and lacks a signaling component [27]. This GPI anchor does not prevent signaling and plays an active role in Ca<sup>+2</sup> mobilization and neutrophil degranulation [25]. Also, CD32A can co-aggregate with CD16B and aid in triggering cytotoxicity although the cross-regulation of this process has not been completely solved [8, 25]. CD16A's ITAM is negatively regulated by CD32B and its ITIM [26]. Another pathway that regulates CD16 is CD32A ligand-binding function, although this too has not been completely solved [8].

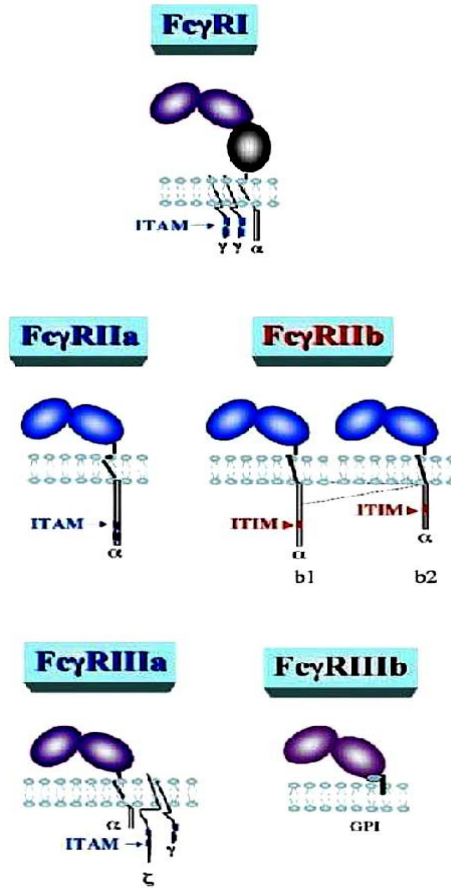


Figure 1. Human Fc $\gamma$ R family of receptors [13]. Fc $\gamma$ RIIC, Fc $\gamma$ RIV are not shown. Figure from Fridman, et al., Immunology 2004. Anchorage is accomplished by single pass polypeptide ( $\alpha$ ) or by Glycosyl Phosphatidylinositol (GPI). Associated signaling pathways are depicted by  $\gamma$  and  $\zeta$ . Fc $\gamma$ RIIa and Fc $\gamma$ RIIb have intrinsic signaling pathways that are incorporated in the  $\alpha$  polypeptide anchor. ITAM (activation) and ITIM (inhibitory) are the signaling pathways depicted.

It should be noted that polymorphisms exist in the Fc $\gamma$ R family [19]. These changes in the structure have been shown to have an effect on receptor binding and have also shown to have an influence in immunotherapy. The three receptors with notable polymorphisms are Fc $\gamma$ RIIA (R131H), Fc $\gamma$ RIIIA (V176F), and the two neutrophil antigen forms of Fc $\gamma$ RIIIB previously mentioned. The expression of the arginine at amino acid position 131 in CD32A, the valine in CD16A, and neutrophil antigen 1 in CD16B all increase efficiency of binding with IgG. There are reports of less frequent

polymorphisms in all members of the FcR family and each has an effect on the binding function of the receptor. Some polymorphisms, like CD16A V176F have been studied in an attempt to find a link to certain autoimmune diseases [19]. The V176F mutation in CD16 is involved in three of the six mutations that have been selected to be expressed in soluble form in this study.

As previously described, Fc receptors play a major role in our body's immune responses and understanding the Fc $\gamma$ R will only further aid our knowledge of autoimmune diseases and antibody-mediated immunotherapy. There is much that is still not known about Fc $\gamma$ R, such as the solved structures of all members of the family (including complex formation with IgG), which are important to understanding this family of receptors as it can be correlated to complimentary functional data. These studies can discover and verify trends among the receptors, be used as a verification method to proposed renderings of structures, show amino acid locations, show both internal and external binding characteristics, and show other molecular structures that may be present. Several groups have published research papers using x-ray crystallography as a method of solving the structures of Fc $\gamma$ R [4, 5, 28, 29, 30].

## **1.2 X-ray Crystallography Technology and History**

X-ray crystallography was accidentally discovered almost 100 years ago when a German physicist, Max von Laue, directed an X-ray beam through a crystal and discovered a diffraction pattern [31]. A few years later, an Australian team of William Henry Bragg (father) and William Lawrence Bragg (son) won the Nobel Prize for Physics by using a mathematical method to analyze the diffraction data put forth by the X-ray. This process, deemed X-ray crystallography soon grew in importance as X-ray diffraction patterns were used to determine numerous molecular models of biological and chemical formations. First used to determine atomic structures in biochemical materials,

the technique has grown to play a role in synthesizing medical chemicals, mineralogy, and in our case, protein structures. X-ray crystallography of DNA, performed by Rosalind Franklin, played a large role in James Watson and Francis Crick's solution of the DNA double helix structure. The first protein crystallized and solved was myoglobin from a sperm whale (1958) [32].

X-ray crystallography technology has improved vastly in the past 15 years, allowing for far superior resolution in solving proteins to the point that amino acids, solvents, sugars, and other structures can be readily determined. In order to determine a protein structure, a large amount of pure protein must be developed and a crystal must form with the protein inside of it [32]. A vapor diffusion method was used for growing crystals in this project [79]. This method uses a closed chamber with a large reservoir with precipitant solution and a hanging drop above that is made of equal parts protein solution and the reservoir solution. The precipitant level in the drop increases and may force crystals to form as a vapor reaction takes place, pulling the water out of the drop.

Once crystals are formed, an X-ray diffraction experiment is set up. An X-ray source generates an X-ray beam that passes through the crystal and becomes diffracted. The X-ray beam is filtered by monochromators and/or mirrors, which create a more focused X-ray beam and a better pattern by lowering background interference [78]. The crystal itself is mounted on an apparatus that is rotational [77]. The diffraction pattern is recorded on the opposite side of the crystal and further analyzed in order to determine the structure. This experiment will make use of molecular replacement software with a previously solved protein, sCD16B<sup>NA2</sup>, as a template. After exposure, the crystal can be become damaged due to the onset of chemical reactions triggered by the beam. Using a high power source like a Synchrotron will give better results before the crystal is too damaged to be accurate [78]. Proteins are asymmetric objects and are determined by examining the diffraction pattern and taking note of any symmetry and systemic absences [78]. This gives rise to space groups. There are 230 possible space groups, but only 65

are possible due to the asymmetry. Using space groups and molecular replacement, structures can be developed. Resolution can also be improved by a method that rapidly cools the crystal to a temperature close to that of liquid nitrogen. This process is called cryo-cooling [79].

The limiting step is usually the protein crystal development because the x-ray diffraction patterns tend to be weak, which can be offset by larger crystals containing high amounts of pure target protein with the crystal solvent (about 50%) [76]. Purity of the proteins allow for larger crystal growth as impurities in the solution can create precipitation, create conformation changes to the target protein, affect solubility, and alter solvent conditions to prevent crystals from ever forming. The method is not sensitive enough to obtain a diffraction pattern from just one molecule of the protein but can obtain significant patterns when the starting protein solution is of the milligram per milliliter concentration [77].

### **1.3 Structure Studies of the FcγR Family**

The FcγR family has been undergoing crystallographic analysis by several groups [4, 5, 28, 29, 30]. These studies include the structures for FcεRIα (Garman and Wurzburg et al [33]), FcγRIIA (Maxwell et al [29]), FcγRIIB and FcγRIIIB (Sondermann et al [4, 30], and a second FcγRIIIB (Zhang and Sun et al [5]). Results from the crystallographic analysis, combined with sequence analysis, show about 40% sequence similarity between these receptors, a general heart shaped form, and high interaction between the Ig domains [34]. These studies are major influences in this current project are described next.

FcεRIα is the high-affinity IgE receptor [34] and it is found on the surface of effector cells [28]. These effector cells are involved in several processes, including allergic responses, anaphylaxis and anti-parasitic immunity. The receptor has a Kd of  $10^9$  to  $10^{10}$  and is either a trimeric or tetrameric form [35]. Crystal structures of this

receptor were formed alone [28] and as a complex of IgE-Fc-FcεRIα [33]. Figures 2 and 3 show these forms. Garman first developed the receptor alone and then later bound to IgE-Fc, but needed to make residue substitutions to the IgE-Fc protein in order to improve the crystal qualities [35]. Insect cells were used to express wild type IgE-Fc, FcεRIα and a carbohydrate mutant, FcεRIαΔ4-6, which lacks three of the seven wild type carbohydrate sites and was developed to improve crystal formations [35]. After the complex formed, vapor diffusion was used to form the crystal, which took 1 year to appear, before diffraction and modeling took place [36]. The complex made with wild type FcεRIα receptor had a limiting resolution of 4.5Å, while the carbohydrate mutant (Δ4-6) showed a limiting resolution of 3.5Å [35].

The model for FcεRIα (Figures 2A and 3A) shows two, non-identical, tryptophan heavy binding sites for IgE-Fc. These binding sites will be explained after the completion of the FcR structure review. These tryptophans bind to prolines in the Fc-fragment. Site 1 shows two potential salt bridges and four potential hydrogen bond sites, while site 2 shows three potential hydrogen bond sites [28]. The FcεRIα- IgE-Fc binds in a 1 to 1 ratio due to conformational changes in the linker region of IgE-Fc upon complex formation and the blocking of further receptors by steric hindrance [35, 37]. Garman suggests that a kinetic scheme can be developed because there are two binding sites [35]. He also calls attention to a study by Sayers, et al [38], that shows a biphasic disassociation rate for the two binding sites and that drug therapy could exploit this. The study and model show good results, but the limiting resolution and mutations still don't give a perfect model. Overall, the FcεRIα- IgE-Fc complex (Figure 2B) is very similar to the FcγRIIB-IgG-Fc interaction (Figure 3B) and is a valuable source of information for studying FcγR receptors.

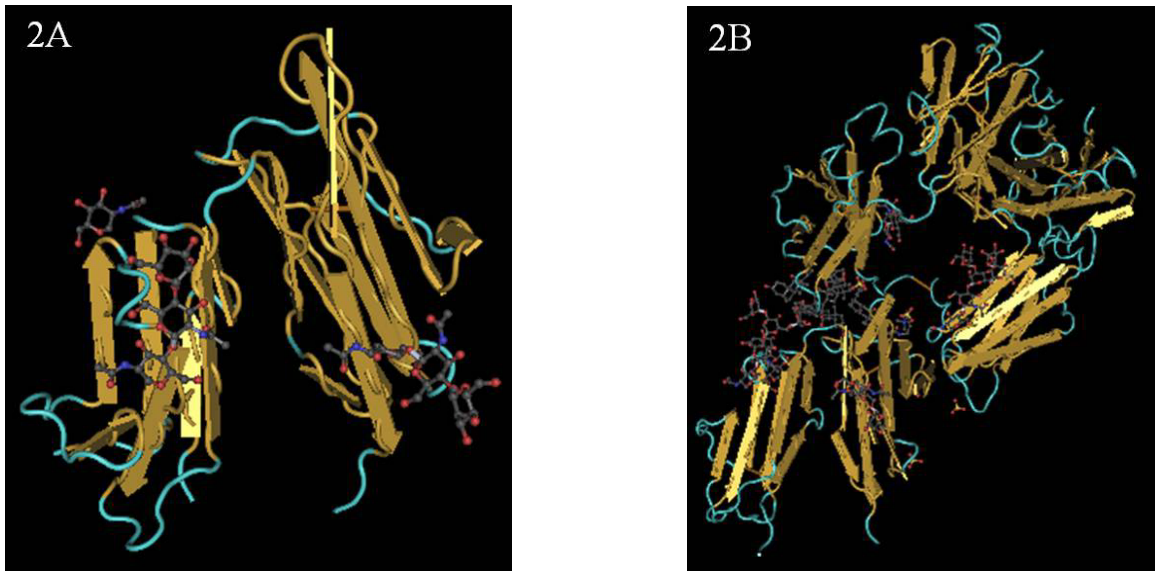


Figure 2. Solved crystal structures of FcεRIα, 2A, (MMDB #13689, PDB #1F2Q) [28], and of the FcεRIα- IgE-Fc complex, 2B, (MMDB # 13872, PDB #1F6A) [33], from Entrez Molecular Modeling Database (MMDB) [71].

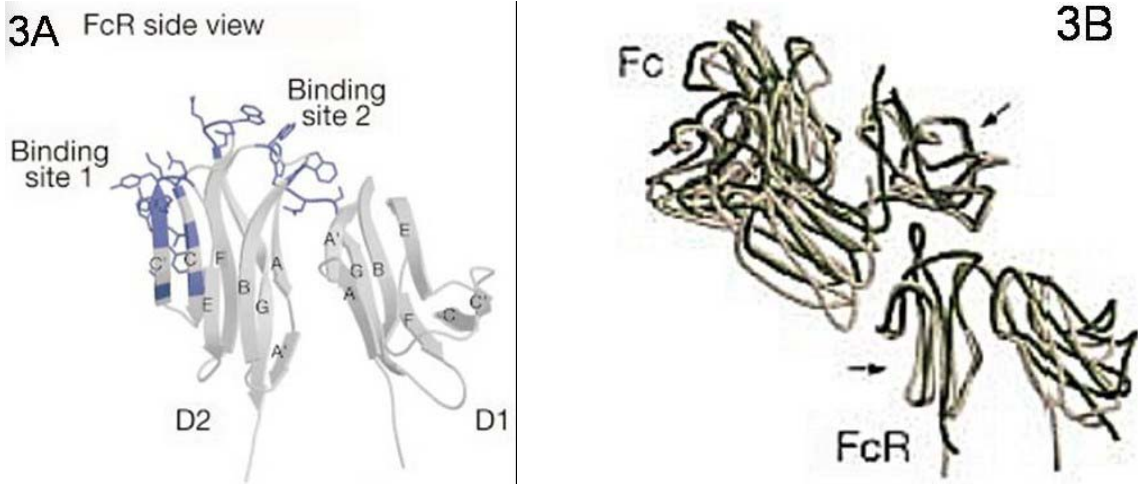


Figure 3. Side view of FcεRIα in ribbon form, 3A. Binding residues are in stick form while strands are labeled [33]. Superposition of FcεRIα -IgE-Fc complex (beige) with FcγRIIB-IgG-Fc complex (green), 3B. Arrows indicate domains used to superimpose complexes [33]. Figure from Garman, et al. (MMDB #14309, PDB #1FP5) [33].

Kelley Maxwell (Biomolecular Research Institute) and Maree Powell (Austin Research Institute) produced the crystal structure and model for Fc $\gamma$ R1IA in 1999 [29]. Their study obtained a 2.0 Å resolution structure of the extracellular portion of CD32A (Figure 4a). Human Fc $\gamma$ R1IA was developed [39] by both mammalian and insect cell methods to form the appropriate crystals needed for trials. There was difficulty in the interpretation of the diffraction data and modified phases used only 76% of the amino acid residues to start the solving process [29]. After several cycles of refitting the structure was finalized. Even with the 2.0 Å resolution, the authors admit that some of the residues' atomic positions cannot be considered totally reliable [29]. This in itself is reason enough to garner more attention to Fc $\gamma$ R crystal studies.

Maxwell and Powell's study showed several things about the CD32A structure. They calculated a 52° angle between the domains (D1 and D2) [29], which is similar to the previous Fc $\epsilon$ RI structure [28] and backed up by sequencing studies showing the conservation among the receptors [29]. The model also showed that D2 was the main ligand binding domain and had a two residue linker to D1. This structure also had several potential hydrogen binding sites in its contact area. Past research [40] using substitution mutations to define the binding region for IgG1 was repeated for IgG2 to confirm the main ligand binding region [29]. An exposed Arginine at position 134 in D2 is the reason that the receptor is shown to bind IgG1 and IgG2 differently [29]. One of the main features that this study found was CD32A formed dimers (Figure 4b) in the crystal structure that were very similar to those found in the V<sub>L</sub>V<sub>H</sub> structures (light and heavy chains of the antibody variable domain) [41], although it is a tighter pack. The study predicts that this dimer formation is involved in the binding of IgG and that the other CD32 subunits are similar due to the similarity of the extra-cellular sequencing [29]. The results of this study are in contrast with Peter Sonderrmann's findings [30] which are to be discussed next.

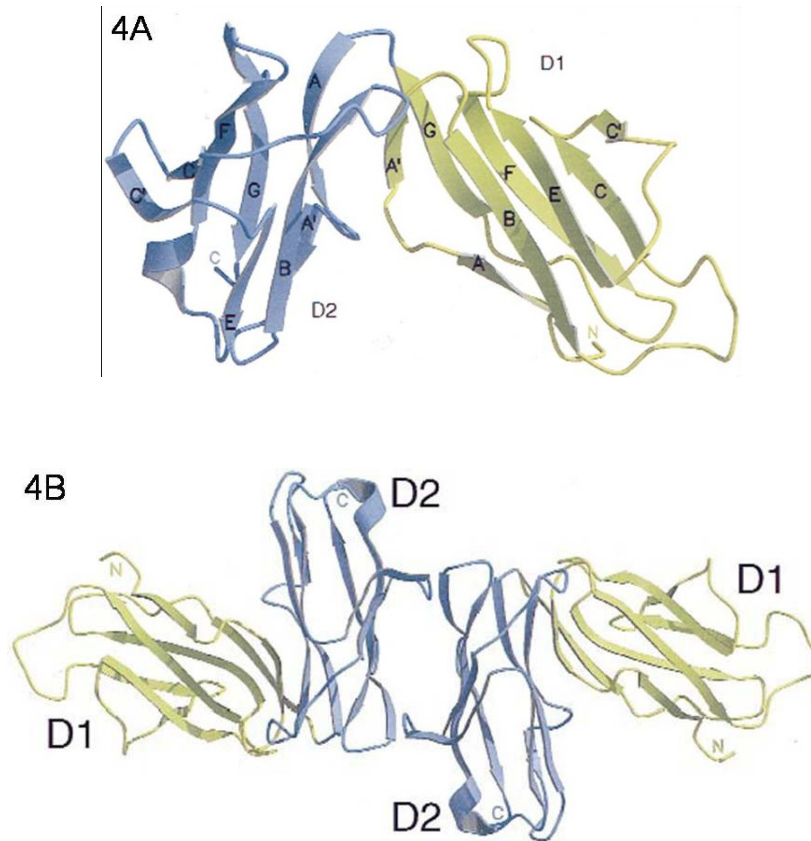


Figure 4. FcγRIIA structure, 4A, in ribbon form. Strands are lettered A-G while D1 domain is blue and D2 domain is green with an angle of 52° between them. Ribbon diagram of an FcγRIIA dimer, 4B. Figure from Maxwell, et al. (MMDB #13259, PDB #1FCG) [29].

Peter Sonderrmann and colleagues solved the crystal structure of FcγRIIB [30] to a limiting resolution of 1.7Å in 1999. The author developed recombinant soluble (extracellular) human CD32B and expressed the protein in *E. coli* cells. An Inclusion Body method, described in detail later, is prepared by a sonication method from overexpressed extracellular CD32B [42]. After dissolving the inclusion bodies and refolding the proteins, crystals were formed using a vapor diffusion method. Diffraction data was collected and an electron density map was formed to 2.1Å and later to 1.7Å with several model refinements [30].

Sonderrmann's CD32B (Figure 5) structure is made of two domains forming a heart shaped sandwich with a 70° angle between the two domains [30]. Three different

spacing groups resulted in the same structure, confirming its reliability. However, all three groups showed disorder of the last nine residues of the polypeptide chain [30]. The structure also found three potential N-glycosylation sites: N61, N142, and N135. The study suggests from further computer modeling that two CD16B receptors bind to a single antibody forming a 2 to1 stoichiometry. It is also suggested that this model creates an upright complex allowing for further binding that would help explain the signaling capabilities of the receptor. This is obviously in disagreement with the CD32A crystal study and provides more reason for further crystal studies.

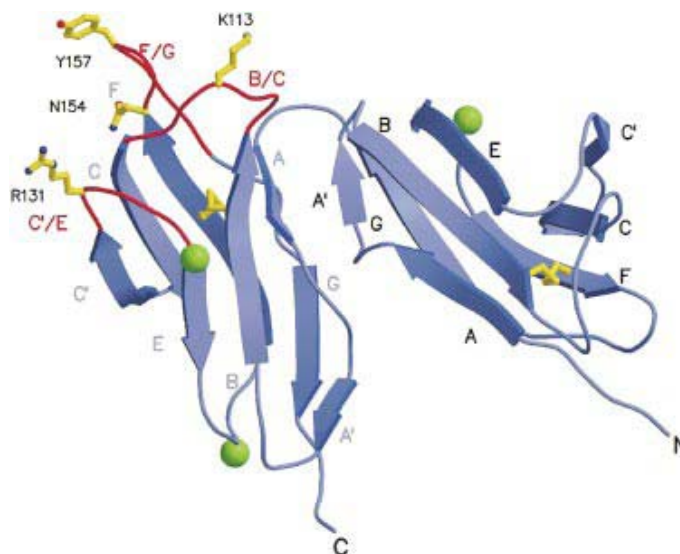


Figure 5. Structure of human sFcγRIIB in ribbon form. Red loops are interaction sites for IgG binding. Ball and stick formations are key residues for IgG binding and the disulfide bridge. Green Balls are potential N-glycosylation sites. Figure from Sondermann, et al. (MMDB #12664, PDB #2FCB) [30].

The final crystal structure studies and the most relevant for our project are Peter Sondermann, et al. [4], and Peter Sun, et al. [5]. These recently published papers report the crystal structures of FcγRIIB bound in a 1 to 1 complex with human IgG1 Fc. Sondermann was able to show the bound structure at a 3.2 Å limiting resolution (Figure

6A and 6B). Upon the binding of sCD16B, hFc1 undergoes a structural reorganization (Figure 7). C $\gamma$ 2 moves away from C $\gamma$ 3 upon this reorganization, along with a similarity between the Fc $\gamma$ R's and the "Proline sandwich" being the primary binding motive in FcR-Ig complexes, provide Sonderrmann with a proposed mechanism for an allosteric interaction between FcRn's and Fc $\gamma$ R's using antibodies. The two C $\gamma$ 2 domains change differently, while C $\gamma$ 3 remains relatively unchanged during this reaction. Pro 329, an amino acid that is involved in the "proline sandwich," moves C $\gamma$ 2-B a further distance away than C $\gamma$ 2-A. The sCD16B also undergoes a significant change upon the binding furthering his mechanism. Sonderrmann found that the interdomain angle increased 10°, from 70° to 80°. There is also a side chain, Trp 95, which comes into contact with Tyr 14 (sFc $\gamma$ II numbering system). The author also goes into the interaction of the amino acids involved in the binding region and the possible van der Waals interactions and hydrogen bonding between them. This seems to be a limiting factor of the study. The limiting resolution of 3.2Å seems to be insufficient for finding these interactions with enough certainty. Also, Sonderrmann only used sCD16B<sup>NA2</sup> in his experiments and there are two forms of CD16B and one for CD16A.

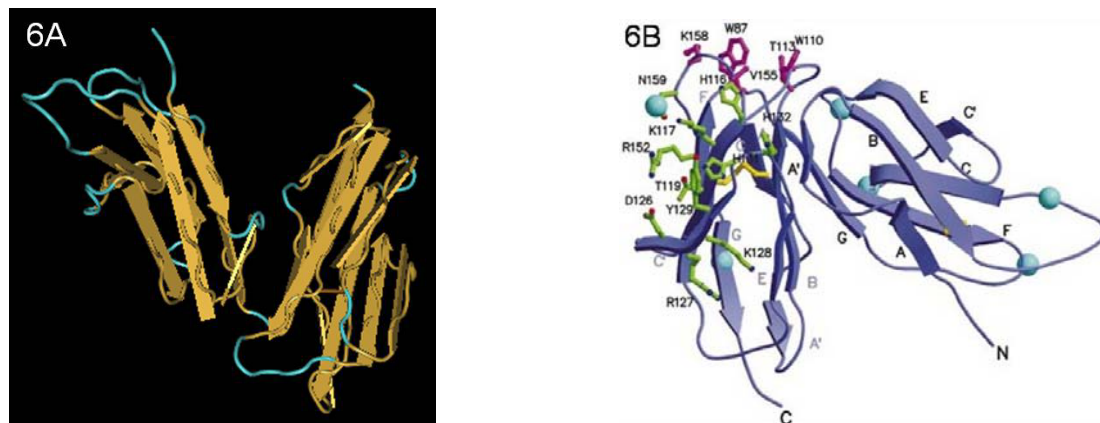


Figure 6. Structure of sCD16B in two forms. sCD16B, 6A, (MMDB #14218, PDB #1E4J) [4, 71]. Stereo ribbon structure of sCD16B, 6B, with IgG contact residues in ball and stick formation. Green contacts C $\gamma$ 2-B while magenta contacts C $\gamma$ 2-A. Large balls (blue) are potential glycosylation sites and disulfide bridge is yellow. Figure B from Sonderrmann, et al. [18].

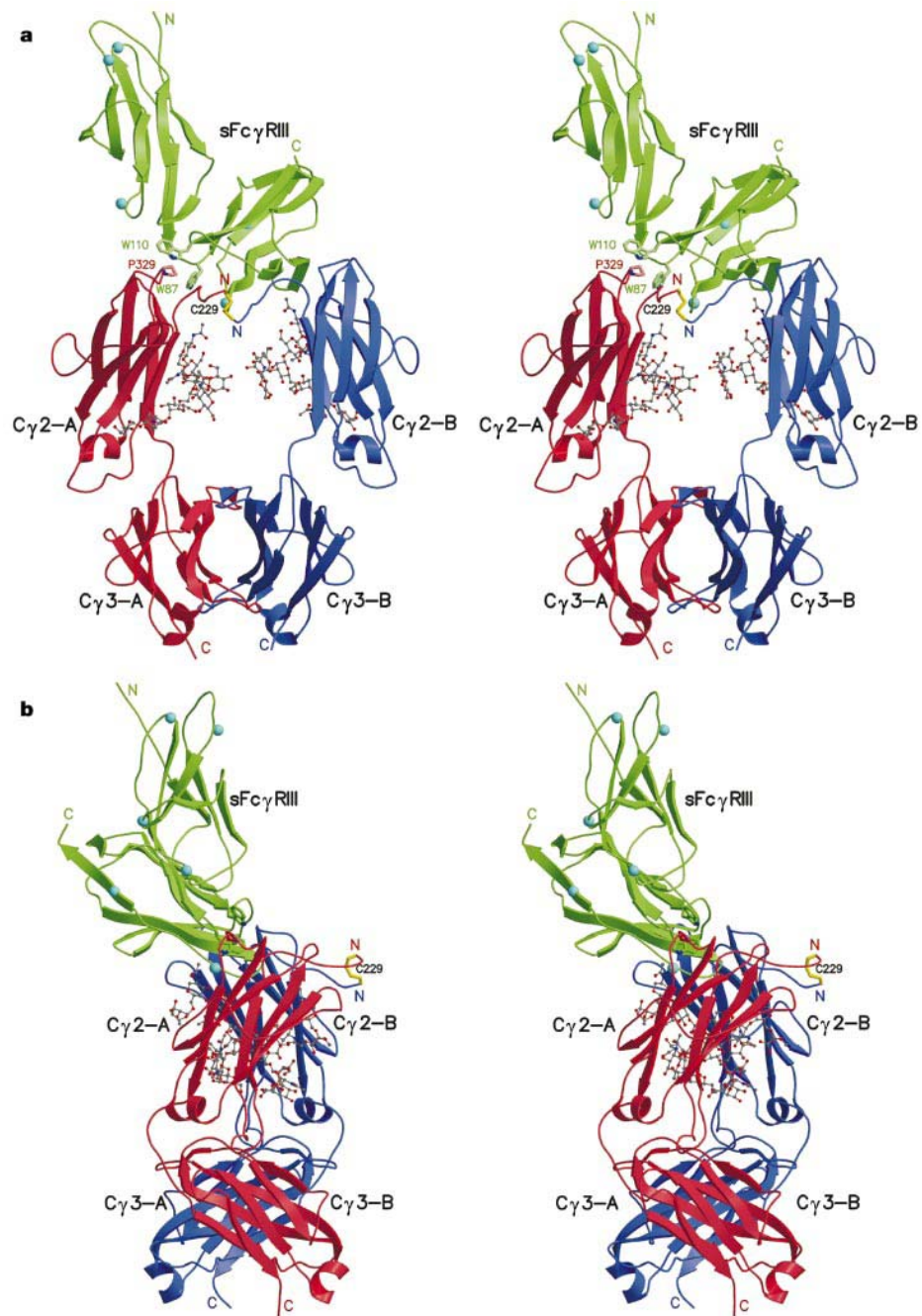


Figure 7. The structure of the sFc $\gamma$ RIII-hFc1 complex in the vertical view, a, and in the 90° rotated side view, b. Ball and stick figures represent the “proline sandwich” while larger blue spheres exhibit glycosylation sites [4]. Figures created by MOLSCRIPT [72]. Figure from Sondermann, et al.(MMDB #14214, PDB #1E4K) [4].

Peter Sun and colleagues [5] focused more on the extracellular portion of the sCD16B molecule (Figure 8) than Sondermann's paper did. The authors, as the previously mentioned paper, showed the conservation of important regions throughout the FcγRs, which demonstrates the importance of solving a possible mechanism for these molecules. This paper solved the crystal form of the sCD16B to a 2.3 Å limiting resolution using a multi-wavelength anomalous dispersion method. The authors were able to refine the model to 1.8 Å resolution using additional techniques (Figure 8A). However, the authors seemed to have used a symmetry method that ended up taking away from the completeness of the molecule and calling into question the exactness of the actual form of sCD16B. Zhang et al. also found the interdomain hinge angle to be 50° which is far smaller than the 70° pre-complex angle reported by Sondermann et al. They noted previous discrepancies of reports of the domain angle of FcγIIA and FcγIIB [6, 7]. These angles were between 52° and 70° are attributed to using different algorithms in solving the structure. Zhang et al. [5] tried to help explain the smaller angle by Domain 1 and Domain 2 being tightly packed together from interdomain interactions, i.e., van der Waals and hydrogen bonding (Figure 8B). Also, he mentions that a bound phosphate ion was found in the hinge region on the second sCD16B molecule and that it has a role in the angle differences (Figure 8D). Peter Sun and colleagues showed further detail than that of Peter Sondermann et al., but both studies need a better resolution in order to see all the effects of sugars, salts, and interdomain interactions.

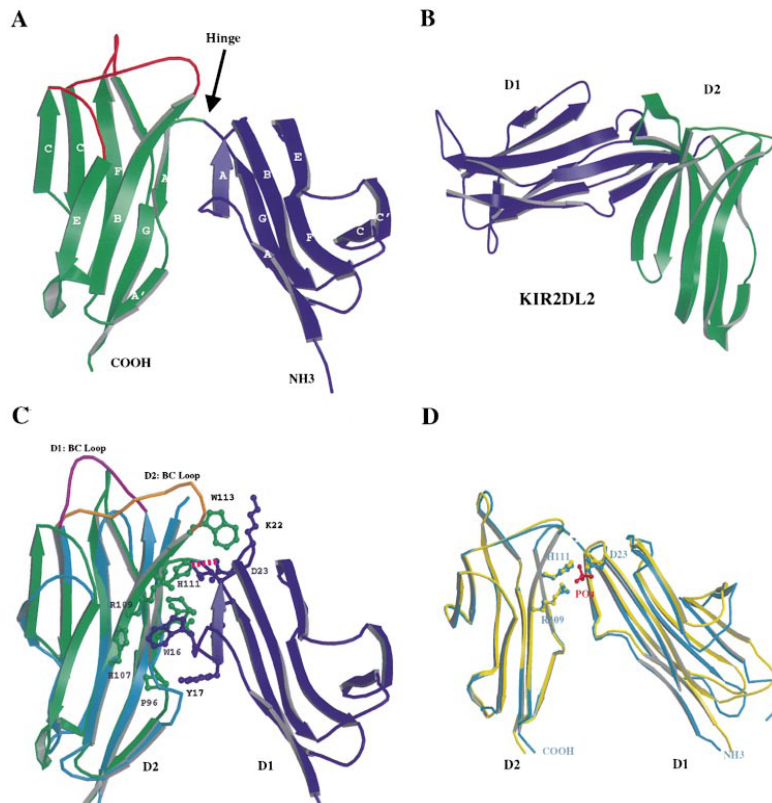


Figure 8. Structure of FcγRIII [5] created by MOLSCRIPT [72]. A, FcγRIII's (ribbon form) binding loops are red, D1 domain is blue, D2 domain is green. B, KIR's domain orientation (ribbon form) resembling FcγRIII. C, FcγRIII's (ribbon form) interdomain region focusing on the packing domains (dark blue and green). Residues and domains are labeled in the figure. D, Asymmetric unit containing superimposed molecules A and B of FcγRIII. Figure from Zhang, et al. (MMDB #14531, PDB #1FNL) [5].

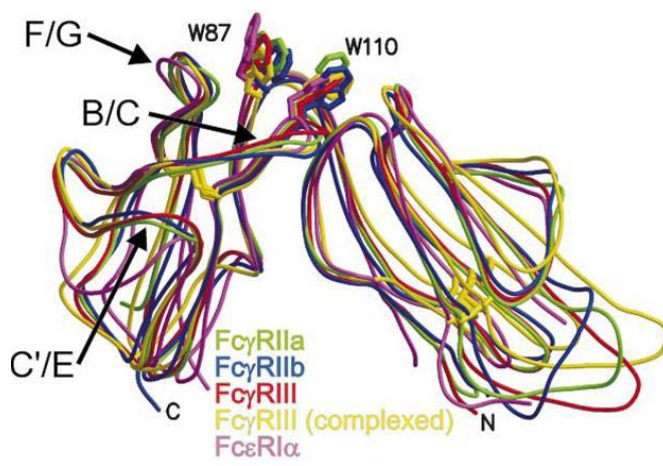


Figure 9. FcR structures superimposed [18]. Disulphide bridges in yellow. The color of the FcR name is the color of the structure. Figure from Sondermann, et al. (PDB #'s 1FCG, 2FCB, 1FNL, 1EFJ, 1F6A) [18].

Using the solved sCD16B<sup>NA2</sup>-IgG complex as a template, Sonderrmann and colleagues [18] proposed that the FcγR-IgG interactions are conserved throughout the FcR family. There are three main regions of the IgG molecule that FcR interacts with. They include the exposed proline at amino acid 329, the Cγ2-A region, and the Cγ2-B region (Figure 7). The binding domains of each member of the FcR family that interact with these three IgG regions are conserved in location but not necessarily in sequence. The binding domains for FcR are located in the B/C, C'/E, and F/G loops. The C' strand also contains important residues. These regions are shown in Figures 2 through 9. The binding residues for FcR are as follows. Trp 87 and Trp 110 are the main binding residues for CD16, CD32, CD64, and FcεRIα. They bind the antibody's Pro329 making a "proline sandwich." The residue at amino acid position 155 is responsible for binding to the Leu235 of IgG. This interaction is not conserved throughout the family. Position 155 is a solvent exposed hydrophobic residue in CD16 and CD32 and leads these receptors to a low affinity interaction. CD64 has a more pronounced hydrophobic interaction with Leu235 by using tyrosine and tryptophan, which accounts for its higher affinity. Leu235 is replaced by a proline in IgE, which interacts with Trp 156 and Leu 158 residues of FcεRIα accounting for its higher affinity.

CD16 and CD32 have additional residues that alter the binding of Leu235. CD16 has three histidine residues that contact residues 234-238 of the Fc-fragment. His131 and His 132 are part of the C'/E loop while His116 is part of the C strand. These residues come into contact with Leu235 and lower the binding affinity. In CD32, the histidine residues are replaced with smaller residues which would allow the Fc-fragment to bind closer to the receptor if not for the arginine at residue 131. This residue lowers the affinity of CD32. The final important residue is at position 129. This is tyrosine in CD16 but may be phenylalanine in the other Fc receptors. It makes multiple contacts with the Fc-fragment and is forces the receptor to tightly bind to the hinge region.

The previously mentioned studies have gathered a large amount of information on the FcR family of receptors. Figure 10 shows a sequencing study of all the wild types in the group and along with the gathered structure data, show conserved regions and residues that are involved in the functional binding [4]. The extracellular domains are also similar enough in 3-dimensional form to create binding schemes and motifs for the entire family. Of particular interest are the interactions between Fc- gamma receptor III (Fc $\gamma$ III or CD16) and IgG antibodies. A large amount of functional studies exist compared to the structure studies. However, much is to be learned about the functional characteristics of the FcR family. To have completely comprehensive functional analysis, high resolution crystal structures of CD16 are needed to help understand the structure-function relationship. The CD16A structure has not been solved yet and its addition would only strengthen the studies of this family. Previous studies have focused on crystal studies of the CD16B<sup>NA2</sup>- IgG Fc complex [4, 5].

This study will focus on the soluble form of CD16A and several site-specific mutations located in the interfacial region of the CD16B<sup>NA2</sup>- IgG Fc complex, which may change the form of the structure and/or its binding capabilities. This information could lead researchers to a better understanding of the FcR family and improved methods to fight autoimmune disease, including drug development targeting these receptors. With improvements in crystallography and prokaryotic expression pathways, the CD16A structure can be solved along with CD16A and CD16B site specific mutants. Resolving all previous structures to a more definite level, both alone and in complex, with a better limiting resolution is also of importance. Finally, carbohydrates and other effects need to be included in these studies in the future as they play an important role in the capabilities and structure of the FcR family. Typically, they are absent from these studies due to a prokaryotic expression system's lack of post-translational modifications when expressing mammalian proteins. Insect cell expression pathways have some post-translation modifications, but are not always identical to the mammalian protein in native form.

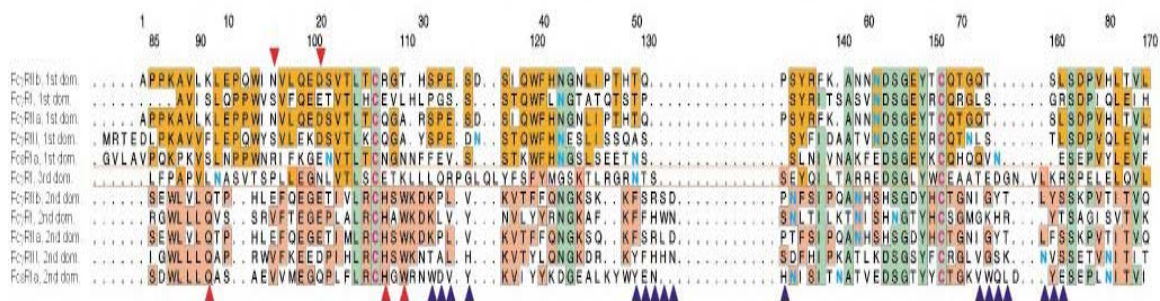


Figure 10. Sequence alignment of the FcR family [4] created by ALSCRIPT [73]. Magenta depicts conserved cysteines. Potential glycosylation sites are in blue. Orange depicts identical residues in the first domain, while those identical in the second domain are pink and those identical in both are green. Contact between domains by way of residue side chains are depicted in red arrows, while blue arrows are binding contact to IgG. Figure from Sondermann, et al. [4]

## CHAPTER 2

### MATERIALS AND METHODS

#### 2.1 Construction of the Soluble CD16 Gene

DNA for wild type CD16A [43] and six site specific CD16A and CD16B mutants were obtained from Dr. Torsten Witte in *E. coli* cells (Invitrogen's TOP 10) with pcDNA 3.1 vectors. The site specific mutants included were sCD16A F176V, sCD16A G147D, CD16B<sup>NA2</sup> V176F, CD16B<sup>NA2</sup> D147G, sCD16 B<sup>NA1</sup> V176F, and sCD16B<sup>NA1</sup> D147G. Cultures were formed from these samples and a portion of each cell line's pellet was diluted in fresh liquid broth and grown at 37° C on agar plates with Ampicillin (100 µg/ml concentration) for colony selection. Selected colonies were grown overnight in 5 ml of liquid broth with Ampicillin at 37°C. A Qiagen Quickspin Miniprep Kit was used to obtain purified gene and vector DNA for all 7 CD16 protein cell lines. Restriction digestion and gel electrophoresis were used to verify results [43].

Primers were developed [50] to insert a stop codon after amino acid Ser-211, as well as two restriction enzyme sites, Not I and Nde I. The forward primer is named CD16extFP. The 5' to 3' sequence is TGTGGCCAT**ATG**TGGCAGCTGCTCCTCCCA (start codon is underlined and the Nde-I site is in bold). The reverse primer is named CD16RPextnotI. The 5' to 3' sequence is CCCAG**CGGCCG**CGAATT**ATG**GAGATG GTTGACACTGCCAA (stop codon is underlined and the Not-I site is in bold). Once in place, the new gene will now produce the soluble portion (extracellular) of the CD16 protein from amino acid 2 to amino acid 211.

The soluble portions of all 7 CD16 proteins were replicated using Polymerase Chain Reaction (PCR) [50]. This reaction uses heating and cooling to open up the DNA

and primers along with polymerase to target a portion of DNA and replicate it. The target DNA will be replicated exponentially due to repeated heating and cooling steps. The setup of the PCR reaction is as follows. Each individual reaction has 10 µl of 10x PCR buffer (High fidelity grade- Invitrogen), 1.5 µl of forward primer, 1.5 µl of reverse primer, 10 µl of template DNA (1 to 4 ratio of DNA to water), 1 µl of dNTP, 0.75 µl of Platinum Taq Polymerase Hifi (Invitrogen), 10 µl of MgCl<sub>2</sub>, and 65.25 µl of sterile distilled water. PCR products for all seven proteins were purified in a PCR purification kit from Qiagen (Qiaquick PCR Purification Kit) [66].

The soluble proteins were ligated to a new vector, pET-21a+ (Novagen) [50]. The new vector and the soluble proteins are first digested with Nde-I and Not-I (Figure 11) [54]. This reaction contains 10 µl of purified PCR product, 6 µl of sterile distilled water, 2 µl React 3 buffer (Invitrogen), 1 µl of Not-I (Invitrogen), and 1 µl of Nde-I (Invitrogen). The solution is mixed in a microcentrifuge tube and incubated in a 37°C water bath for 2 hours. An additional tube is set up that includes 10 µl of pET vector in place of the purified PCR products.

A 1.2 % low melting point agarose gel (Sigma) with Ethidium Bromide (3 µl per 100 ml) was made with 20 µl wells and loaded with the digested products [51]. Gel electrophoresis was run to separate the digested products through the agarose gel. The appropriate soluble protein and pET vector bands were cut out using a UV light and a razor blade. A Qiagen Gel Extraction Kit was used to dissolve the agarose gel and purify the DNA [52, 53].

A Rapid DNA Ligation Kit (Roche) was used to ligate the purified and digested soluble proteins with the purified and digested pET vector (Figure 11) [54, 55]. The protocol includes creating a solution of 3 µl of the insert, 1.5 µl of the vector arms, and 5.5 µl of 1x DNA Dilution Buffer. 10 µl T4 DNA Ligation Buffer (2x concentration) and 1 µl T4 DNA Ligase, was supplemented with the previous solution and incubated for 5

minutes at 15- 25°C. Solutions were stored overnight at -20°C or used right away in a transformation experiment. 4 µl was the typical amount for packaging.

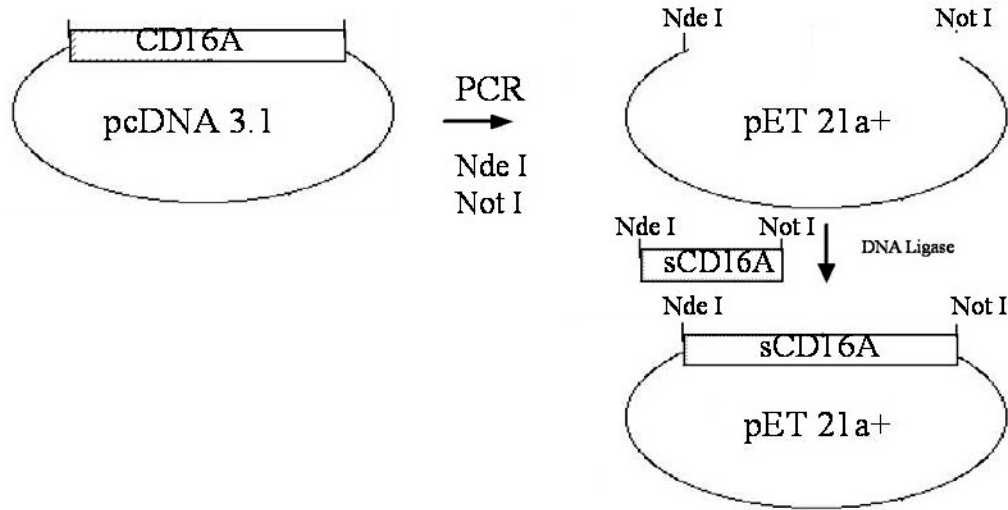


Figure 11. Construction of soluble CD16 gene and insertion into the pET 21a+ vector.

Transformation into TOP10 *E. coli* cells (Invitrogen) was performed next in order to check the success of the previous steps and for long term storage of cells [54]. 4 µl of ligation solution was used in the transformation process. The protocol is as follows [58]. One 50 µl vial of competent cells was thawed on ice per ligation reaction product. 4 µl of centrifuged ligation reaction product solution was added to the competent cells and mixed by tapping gently. The mixture incubated on ice for 30 minutes. The solution was heat-shocked for exactly 30 seconds in a 42°C water bath. The vial containing the mixture was stored on ice and 250 µl of SOC medium (growing medium included in the Invitrogen kit, pre-warmed to 37°C) was added to the solution. The vial was placed on its side in a 37°C shaker and incubated for 1 hour at 225 rpm. 50 µl of incubated solution was spread on agar plates containing Ampicillin (100 µg/ml). The plates were inverted

and grown overnight at 37°C. Colonies were selected (minimum of 5 per sCD16 DNA sample) and grown in 5 ml of liquid broth overnight at 37°C at 225 rpm [54].

Purified DNA was obtained by using a QIAprep Miniprep Kit [57] on 1 ml samples of the overnight growth in the previous experiment [54]. This DNA was used to confirm the success of the PCR, ligation, and transformation experiments. An enzyme digestion was performed on 10 µl of the miniprep product, as previously described, using Not-I and Nde-I [54]. After the completion of this experiment, gel electrophoresis was carried out on a 1% agarose gel with EtBr to separate the DNA fragments [54]. A band at approximately 674 base pairs confirmed the correct restriction enzyme placement, as well as the correct inclusion in the pET vector. A portion of the miniprep, both primers, and the vector were sent off to an outside sequencing lab, which confirmed that the protein was in sequential order.

After proper sequence confirmation, another transformation experiment was performed with cells that contained the proper expression pathway. Since a pET vector was being used, Invitrogen's BL-21 AI One Shot E. coli cells were used with the identical protocol as the previous transformation experiment [54, 56, 58]. Colonies were again selected and grown overnight at 37°C and 225 rpm. Proper transformation was verified by Miniprep DNA purification, restriction digestion, and gel electrophoresis. An alternative expression pathway, Stratagene's BL-21 RIPL [59] was also used when the Invitrogen pathway did not yield high expression for some of the mutants after numerous expression experiments were attempted. The transformation protocol is identical to Invitrogen's TOP10 One Shot tubes and was carried out accordingly [54, 56].

## **2.2 Expression of sCD16 proteins**

The wild type sCD16A was used to establish a basis for expression conditions in both pathways, BL21-AI and BL21 RIPL, as optimal expression conditions are different

for every protein [67]. Both pathways [56, 59] have almost identical protocols for expression [4, 5, 56, 59] with Invitrogen's BL-21 AI pathway having one additional reagent used to turn on the induction pathway. Seed cells were grown overnight (liquid broth inoculated with cells from each pathway grown at 32°C and 225 rpm for 12-16 hours) in order to have fresh cultures for expression experiments [54]. Seed cells were diluted with fresh liquid broth (1 to 20 dilution) and grown until the optical density at 600 nm reads 0.4, signifying that the cells were in log phase, which was the standard point for bacterial induction. To induce sCD16 production, .2% Arabinose and 1 mM IPTG were added to the vessel containing BL21-AI [56]. The vessel containing BL-21 RIPL received only 1 mM IPTG [59]. After 6 or more hours of incubation, each pathway's cells were then spun down at 6,000 rpm and the pellets were collected and the cells lysed. Soluble CD16 proteins were found exclusively in inclusion bodies [4, 5, 50], which were treated, washed, and dissolved to check the protein levels and prepare for refolding. The Inclusion Body Treatment protocol will be in the following section.

After BL21-AI was found to be the preferred pathway (discussed in the results section), more induction experiments were performed in order to fine tune the process and find optimal conditions. Seed cells, with wild type sCD16A in BL21-AI pathway, were grown overnight and diluted with 50 ml fresh liquid broth in each vessel (with 100 µg/ml Ampicillin concentration) and incubated at 37°C and 225 rpm [54]. The cultures were then grown to multiple Optical Density 600 nm levels, which included 0.4, 1.0, and 1.5 [1, 2, 56]. When the culture reached its appropriate level, 0.2% Arabinose and 1 mM IPTG were added to turn on the induction pathway [56]. Each Optical Density level was grown for multiple durations ranging 6-14 hours [1, 2, 56]. All 15 cultures were spun down and their pellets lysed. The inclusion bodies [1, 2] were treated, washed, and separated in a polyacrylamide gel after SDS-PAGE for analysis. Gel electrophoresis [51, 54] was run at 200 volts for 1 hour in either a 10% or 12% Tris-HCl polyacrylamide gel

(50 µl wells) from Bio-Rad. Coomassie blue stain and Western Blot [51, 54] was performed on the gels to determine which starting conditions worked the best.

Coomassie Blue staining protocol is as follows [54]. Polyacrylamide gel was soaked in Fixing solution (50% methanol, 40% water, 10% Acetic Acid) for 90 minutes upon completion of gel electrophoresis. The gel was then soaked in Coomassie Brilliant Blue Stain (45% methanol, 45% water, 10% Acetic Acid, 1g per 100 ml Coomassie Brilliant Blue powder) for 3 to 4 hours. Finally, the gel was soaked in a Destaining Solution (30% methanol, 10% Acetic Acid, 60 % water) until background became clear and bands were visible.

Western Blot protocol is as follows [51, 54]. Upon completion of gel electrophoresis, a semi-dry blotter was used to transfer proteins from the gel to a nitro-cellulose membrane. A semi-dry blotter used a “sandwich” made up of 3 sheets of filter paper, then the gel, then the nitro-cellulose membrane, then three more sheets of filter paper. The filter paper and membrane were cut to the same size as the gel and soaked in Transfer Buffer (25mM Tris buffer, .2M Glycine, 20% Methanol) for 15 minutes before the semi-dry blotter was run for 45 minutes at 90 mA. After completion of the protein transfer, the membrane was dried for 1 hour and then blocked by soaking it in 5% non-dairy milk powder (diluted in 1x TTBS buffer) overnight at 4°C. The membrane was washed in fresh 1x TTBS buffer three times (15, 5, and 5 minutes). Primary antibody (5 µg/ml concentration) was diluted in 1x TTBS buffer. The primary antibody used for sCD16 in the western blot was the anti-CD16 monoclonal antibody, 214.1. The membrane was soaked in this solution for 1 hour at room temperature. The membrane was washed three times again upon completion. A secondary antibody, goat anti mouse, was diluted in 1x TTBS buffer (1 to 1000 dilution). The membrane was now incubated in this solution for 1 hour at room temperature. The membrane was washed, again, with fresh 1x TTBS buffer upon the completion of incubation. Amersham ECL Western Blotting Detection Reagent (GE Healthcare) was used to prepare the membrane for band

development. The membrane was soaked in the Detection Reagent for 60 seconds and then placed with a sheet of unexposed film in an x-ray cassette. X-ray exposure time varied. A typical time for this experiment was 30 seconds prior to developing.

### **2.3 Obtaining and Treating sCD16 Inclusion Bodies**

After optimizing the expression conditions, the wild type sCD16A and the site specific mutants were expressed on a larger scale. After proteins were expressed, the culture was spun down and its pellet collected for inclusion body treatment [1, 2]. The pellet was washed with 1x PBS and re-spun. The following protocol was based on the collected pellets of 6 L of starting culture. The pellet was resuspended in 60 ml of Resuspension Buffer, or Lysis Buffer. This buffer included 50 mM Tris-HCl (pH 8.0), 100 mM NaCl, 5 mM EDTA, 0.1% NaN<sub>3</sub>, 0.5% Triton X100, 0.1 mM PMSF, and 1 mM DTT [1]. The pellet was dispersed in this solution and a stir bar was used to keep the solution flowing. Next, 1.2 ml of 100 mg/ml lysozyme, 300 µl of 1.0 M MgCl<sub>2</sub>, and 1.0 ml of 2 mg/ml Dnase I were added to the solution and left to stir for 30 minutes [2].

Following the resuspension steps, a sonicator was used to send sonic waves throughout the solution [1, 2]. The solution was kept on ice as the temperature would increase the longer the sonic waves were sent into the liquid. There were five rounds of sonication. During each round, the solution was sonicated, on high setting, for 9 minutes total. These 9 minutes were broken up into 90 second intervals of continuous sonication allowing the solution to cool in between each interval [2]. After each round, the solution was centrifuged at 12,000 rpm. The pellet was resuspended in fresh Resuspension Buffer and another round of sonication commenced. The supernatants were saved for future analysis. After the fifth round, the pellet formed after centrifugation was resuspended in Final Wash Solution. The Final Wash Solution contained 50 mM Tris-HCl (pH 8.0), 100 mM NaCl, 5 mM EDTA, and 0.1% NaN<sub>3</sub>. The solution then underwent one more round of sonication and centrifugation. An alternate sonication technique that was attempted

consisted of shorter bursts of sonication waves (30 second intervals rather than 90 seconds) in order to keep the temperature of the solution to a minimum but was discontinued when inclusion bodies were not being washed to an optimal level (discussed in the results section) [1].

The pellet was made up entirely of washed inclusion bodies, which were dissolved so that refolding experiments could take place. The inclusion bodies were dispersed in a Urea solution [1, 2]. The Urea solution contained 100 mM Tris (pH 8.0), 50 mM Glycine, 8.5 M Urea, 5 mM GSSH, and 0.5 mM GSSG. Approximately 100 ml of Urea solution were used for every 2 liters of starting culture. After dispersing the pellet, the inclusion bodies were dissolved overnight using a stir bar at 4°C. SDS-PAGE, followed by gel electrophoresis and a coomassie blue stain, were performed the following day on the dissolved inclusion bodies and the saved supernatants from the sonication steps to check protein purity. Protein concentration in the Inclusion Bodies was estimated by UV scan. Dissolved inclusion bodies were then used in refolding experiments with excess frozen for storage [1, 2].

#### **2.4 Refolding and Concentrating sCD16 Protein From Dissolved Inclusion Bodies**

Refolding of sCD16 was accomplished by a rapid dilution injection [3, 70] of 100 mg of inclusion bodies into 1 liter of Refolding Buffer [3]. The Refolding Buffer included .4 M L- Arginine, .1 M Tris, 5 mM GSSH, .5 mM GSSG, .2 M PMSF (pH 8.3). The buffer was first chilled to 4°C and then an injection of equal volume dissolved inclusion bodies (Urea solution) and Injection Buffer (3 M Guanadine-HCL, 10 mM Sodium Acetate, 100 mM EDTA), equal to 50 mg of protein, was injected into the Refolding Buffer as close to the stirring bar as possible [3]. Stirring continued overnight and a second identical injection was given to the buffer the following morning. Stirring continued another twenty-four hours, at which time the protein has finished refolding.

Once the proteins have refolded, the solution was concentrated to a lower volume using an Amicon stir cell (Millipore) with a 10 kD NMWL Ultracel Amicon UltrafiltrationDisc membrane (Millipore) [4]. Once the solution was concentrated down below 50 ml, then 10 mM Tris or 1x PBS was added to dilute all refolding agents in the solution. After appropriate washing was finished, the solution was transferred to Pierce iCON Concentrator Tubes (9 kD NMWL filter) for completion of concentration to a volume between 1-10 ml. Centrifugation was carried out at 3,000 rpm (4°C) after washing the storage glycerin out of membrane with sdH<sub>2</sub>O [60]. Concentration was carried out to preference, about 3 ml in this case. Refolded protein solution was transferred to a micro centrifuge tube and spun down to rid the solution of all precipitation and aggregates [1]. The final solution was tested for purity by SDS-PAGE, for concentration by Micro BCA Protein Assay Kit (Pierce) [54, 61], and for functionality by Sandwich ELISA [51, 54].

Alternate refolding techniques attempted included a dialysis technique and a size exclusion column with a Urea gradient [70]. Both techniques used the same protein expression and inclusion bodies treatment protocols. The dialysis method [1] involved using SnakeSkin Pleated Dialysis Tubing (Pierce, 3500 MWCO) [62] to slowly lower the Urea concentration, which aids in increasing the yield of refolding [70]. The refolding buffer in this protocol included 0.1 M Tris, 0.4 M L- Arginine, 1 mM EDTA, 1 µg/ml Leupeptin, 1 µg/ml pepstatin, 0.2 mM PMSF, and a particular amount of Urea. The amount of Urea decreased in each step. The first buffer had 4.0 M Urea, followed by 2.0, 1.0, 0.5, and 0.0 M (pH 8.0). The inclusion bodies were added to the dialysis tubing which was clipped or tied off. The tubing and proteins were then submerged into refolding buffer that was stirring to start the dialysis process. Dialysis for each step continued for 24 hours. After the Urea was taken out of the protein buffer and the proteins were refolded, the solution continued to dialyze against a 1 to 4 ratio of refolding buffer (0M) to water for 24 hours. Next, the refolded protein solution was dialyzed

against a storage buffer for 24 hours. This protocol suggested a PNEA buffer (25 mM PIPES, 150 mM NaCl, 1mM EDTA and 0.02% NaN<sub>3</sub>) for the storage buffer [1].

Another refolding method attempted involved the use of a size exclusion column made of Amersham Sephadex beads and a gradient to drive refolding [70]. The protocol for this experiment included the following steps [63, 64]. A chromatography column was packed with Sephadex G-50 beads (1.0 cm x 30 cm) and equilibrated with buffer A (50 mM Tris/HCl, 10 mM MgCl<sub>2</sub>, 100 mM NaCl, 20 mM KCl, 1 mM β-mercaptoethanol, pH 7.5). A 10 ml gradient was created in the column from buffer A to buffer B (50 mM Tris/HCl, 10 mM MgCl<sub>2</sub>, 100 mM NaCl, 20 mM KCl, 5 mM β-mercaptoethanol, and 8 M Urea, pH 7.5). 1 ml of inclusion bodies dissolved in buffer B was loaded in the column and pushed through by the Urea gradient at a rate of 0.5 ml/min. Fractions were collected that contained refolded and separated proteins.

Alternate concentration methods were attempted before using a stir cell. These included using a Centricon Plus-70 (Millipore) [65] centrifuge cartridges and Pierce SnakeSkin Dialysis Tubing [62] with polyvinylpyrrolidone powder. Both methods were based on the Rapid Dilution refolding method. Using Amicon cartridges was rather simple. The cartridge, Centricon Plus -70 ml, was equilibrated with either 10 mM Tris or 1x PBS (sterile). After equilibration, the refolded protein solution was added to the cartridges and spun at appropriate speed. The cartridge cannot be spun faster than 3,000 rpm as the force rendered the membrane useless and protein passed through and/or precipitated. The same cartridge was used up to four times. After the solution was concentrated down to a small enough level, 10- 50 ml, a cartridge that handled a smaller level of solution, the Pierce 7 ml iCON Concentrators previously mentioned, were used to concentrate down to less than 10 ml.

The second alternate method used the same type of dialysis tubing previously mentioned, Pierce SnakeSkin 3000 NMWC [62]. The refolded protein solution was added to the tubing and the tubing was tied, or clipped, so that no leakage occurred.

Polyvinylpyrrolidone (Sigma) powder was spread over the tubing. This powder slowly pulled the water out of the tubing, which concentrated the refolded solution. The process was watched very carefully so that the tubing did not collapse and dry out. Again, the process is stopped at an appropriate level, between 50- 100 ml, so that the previously mentioned Pierce concentrators could be used to finish the concentration. The results of these experiments are included in the next chapter.

## CHAPTER 3

### RESULTS

#### 3.1 Sequencing Analysis of sCD16 Proteins

The wild type sCD16A and four of the sCD16 site-specific mutants were confirmed to have correct sequencing. Sequencing analysis was performed on the protein samples by two different labs and the results were compared to the published wild type. The first laboratory is the Emory DNA Sequencing Facility and is part of the DNA Core Facility at Emory University. The second laboratory is Tom Howard's lab in the Pathology Wing of the Woodruff Memorial Research Building at Emory University. The mutants that had correct sequencing are sCD16A F176V, sCD16A G147D, CD16B<sup>NA2</sup> V176F, and CD16B<sup>NA2</sup> D147G (Table 1, Figure 12). Genes without correct sequencing were not allowed to be expressed. Table 1 shows the sequence locations of the site mutations for both CD16A and CD16B.

Table 1. Mutation sites at amino acid 147 and 176 of sCD16 A and B. Letters in bold are the locations for the site specific mutations involved in this project. Mutations cause the underlined letters to change between amino acids D and G at position 147 and between amino acids F and V at position 176.

CD16 Mutation Sites			Amino Acid 147					Amino Acid 176				
CD16A Sequence	.....	AAA	<u>G</u> GC	AGG	AAG	.....	GGG	CTT	<u>T</u> TT	GGG	.....	
CD16A Amino Acids	.....	K	<u>G</u>	R	K	.....	G	L	<u>F</u>	G	.....	
CD16B Sequence	.....	AAA	GAC	AGG	AAG	.....	GGG	CTT	<u>G</u> TT	GGG	.....	
CD16B Amino Acids	.....	K	<u>D</u>	R	K	.....	G	L	<u>V</u>	G	.....	

Different forms of CD16molecule	CD16Mutants
	CD16-GPI-G147D
	CD16-GPI-F176V
	CD16B-NA1-D147G
	CD16B-NA1-V176F
	CD16B-NA2-D147G
	CD16B-NA2-V176F

Figure 12. Cartoon depicting the locations of the amino acid mutations at position 147 and 176 in both CD16A and CD16B.

### 3.2 Soluble CD16 Expression Pathway Analysis

Two pathways were tested for optimal expression results, Invitrogen's BL-21AI [49] and Stratagene's BL-21 RIPL [59]. Figure 10 shows as SDS-page with Western blot comparing the two pathways after expression and Inclusion Body treatment [1, 2, 54]. BL-21 AI far outperformed BL-21 RIPL when expressing wild type sCD16A for 8 hours at 37° C at a starting Optical Density (600 nm) of 0.4. Cell lysis and sonication treatment steps were the same as previously explained in the Materials and Methods section. The primary antibody used in the Western blot was monoclonal 214.1, while the secondary antibody was goat-anti-mouse. Exposure time was 30 seconds. The Stratagene pathway was still used later in an attempt to obtain a higher expression yield with the sCD16B mutants.

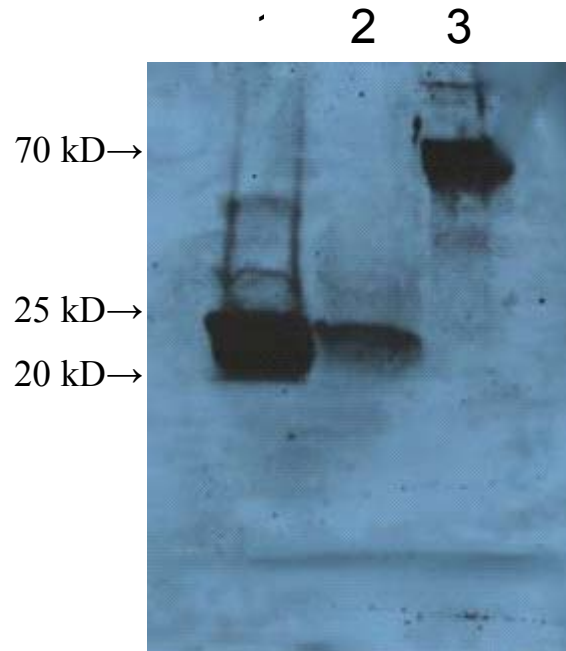


Figure 13. Western Blot analysis on sCD16 induction pathways results after SDS-PAGE. Monoclonal 214.1 was the primary antibody. Lane 1 is sCD16A expressed in the BL21-AI pathway (Invitrogen). Lane 2 is sCD16A expressed in the BL21 RIPL pathway (Stratagen). Lane 3 contains CD16A-Ig complex. Bio-Rad 12% Tris polyacrylamide gel and Bio-Rad nitrocellulose membrane were used.

Expression duration of the proteins and pre-induction initial conditions were tested and found to be optimal when 0.2% Arabinose and 1 mM IPTG are added to the bacterial culture when the solution is at 1.0 OD 600 nm and incubation length continues for 8 hours. Figure 14A shows wild type sCD16A protein levels (SDS-PAGE and Western Blot) at various expression lengths, 4-8 hours. 8 hours outperformed the shorter incubation times for the wild type sCD16A. Figure 14B shows the BL-21 AI pathway when transcription is both blocked and turned on. When Arabinose is added in the appropriate amount, the transcription pathway is turned on as the I<sub>2</sub> inhibitor is blocked (Figure 14B). This pathway was developed by Invitrogen specifically for pET vectors.

The wild type sCD16A and the two sCD16A mutants (F176V and G147) all expressed quality inclusion bodies in the Invitrogen BL21-AI pathway. All three were expressed at an OD 600 nm value of 1.0 with .2% Arabinose and 1 mM IPTG. The two mutant proteins showed better inclusion bodies at 10 hour incubation rather than 8 hour. The two sCD16B<sup>NA2</sup> mutants (D147G and V176F) did not express in the BL21-AI pathway at all. Examples of their expression levels are in Figure 15. Both sCD16B mutants were induced at multiple OD levels and were expressed for multiple durations. The figures show the lack of an appropriately sized band in the low 20 kD range. The Stratagene BL21 RIPL pathway was then used on the two sCD16B mutants in an attempt to obtain the target protein expression. However, this pathway did not produce superior inclusion bodies. Possible reasons for poor expression are included in the Discussion chapter.

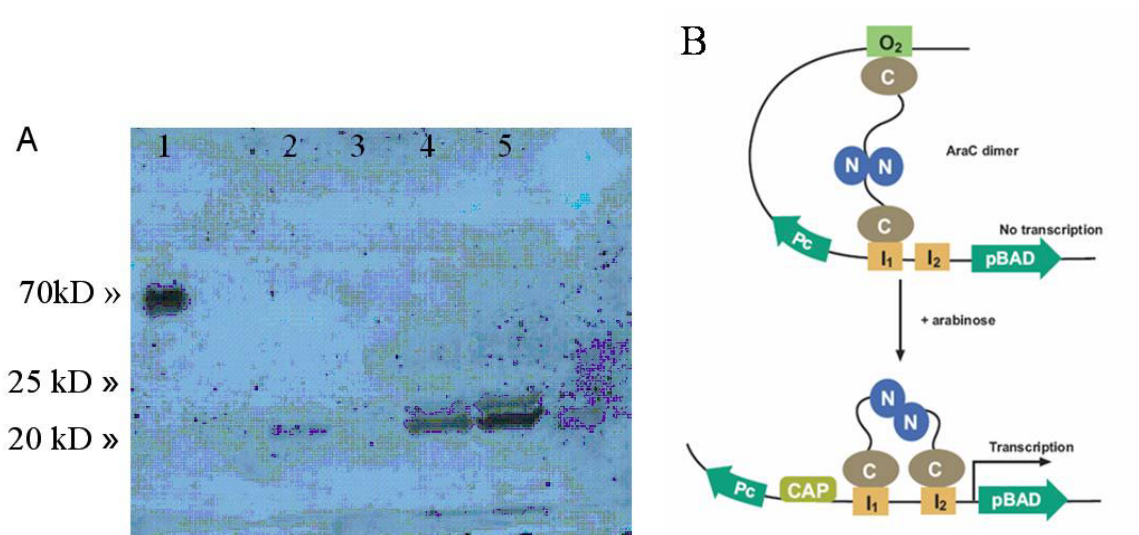


Figure 14. A, Western Blot analysis of SDS-PAGE. Lane 1 contains CD16A-Ig. Lanes 2, 3, 4, and 5 contain sCD16A expressed in the BL21-AI pathway for 4, 5, 6, and 8 hours, respectively. Protein expressed at a OD 600 nm value of 0.4 using 0.2% Arabinose and 1 mM IPTG. B, The expression pathway of BL21-AI (Invitrogen) [49].

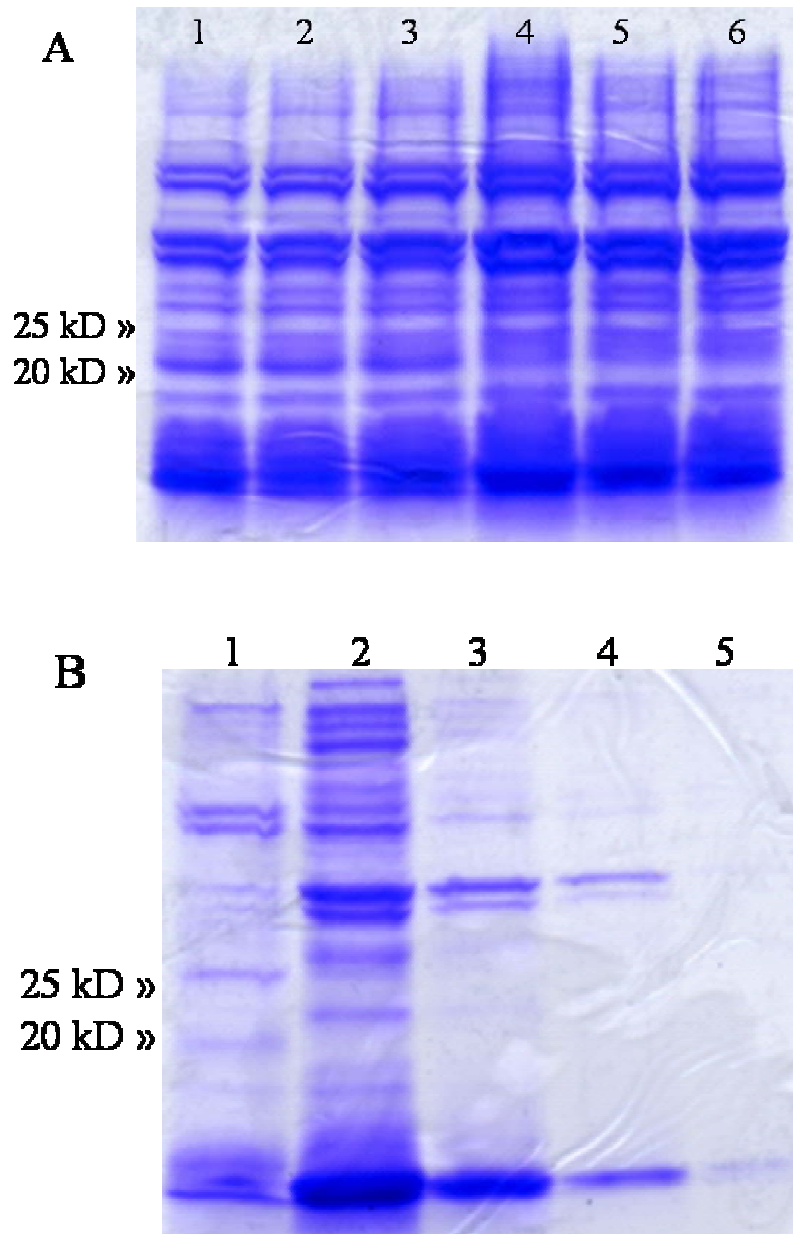


Figure 15. A, sCD16B<sup>NA2</sup> V176F inclusion bodies induced in BL21-AI pathway under different conditions. Lanes 1-3 are induced at 1.0 OD 600 nm, while 4-6 are induced at 1.5. Lanes 1 and 4, 2 and 5, and 3 and 6 were induced for 8, 10, and 12 hours, respectively. B, sCD16BNA2 D147G induced for 10 hours in the BL21-AI pathway at 1.0 OD 600 nm with .2% L-Arabinose and 1 mM IPTG. Lane 1 contains the inclusion bodies, while 2-5 contain sonication supernatants.

### 3.3 Soluble CD16 Inclusion Body Treatment Analysis

Two sonication methods were tested for the quality of the inclusion bodies that they produce. The first was a method by Steinle, et al [1], which included a series of sonication steps with quick short bursts for durations of 30 seconds. The second method, Altman et al [2], included longer durations of sonication, 90 seconds, and slightly different concentration of chemicals (Dnase I and lysozyme are slightly higher and  $MgCl_2$  is substituted for  $MgSO_4$ ) [1, 2]. The following figures (Figure 16) show the quality of the Inclusion Bodies and the supernatants of washing steps. Altman's longer sonication steps showed a cleaner sample compared to Steinle's method (Figure 16C). Figure 16C shows a sizeable target protein band in the low 20 kD range but has far too many non-target proteins in the Urea solution. Figure 16 also shows a lack of target protein in the supernatants as the target protein is found in the inclusion bodies. It also shows the effectiveness of the washing steps as the supernatants are much more clean later in the sonication steps as compared to the initial step.

Inclusion bodies dissolved in the Urea solution typically had a volume of 30 ml and a concentration between 20 mg/ml and 50 mg/ml. The higher the percentage of the target protein compared to the whole of the inclusion bodies, the better the results of the subsequent refolding and purifying experiments [2, 54]. Figures 16A and 16B show quality, high ratio inclusion bodies, while Figure 16C shows poor inclusion bodies in which the target protein makes up a small percentage of the entire sample. Three proteins provided quality inclusion bodies. These proteins are wild type sCD16A, sCD16A GPI F176V, and sCD16A G147D (Figure 16A and 16B). Two mutants, sCD16B<sup>NA2</sup> D147G and sCD16<sup>NA2</sup> F176V, never produced high quality, target protein rich inclusion bodies in either expression pathway.

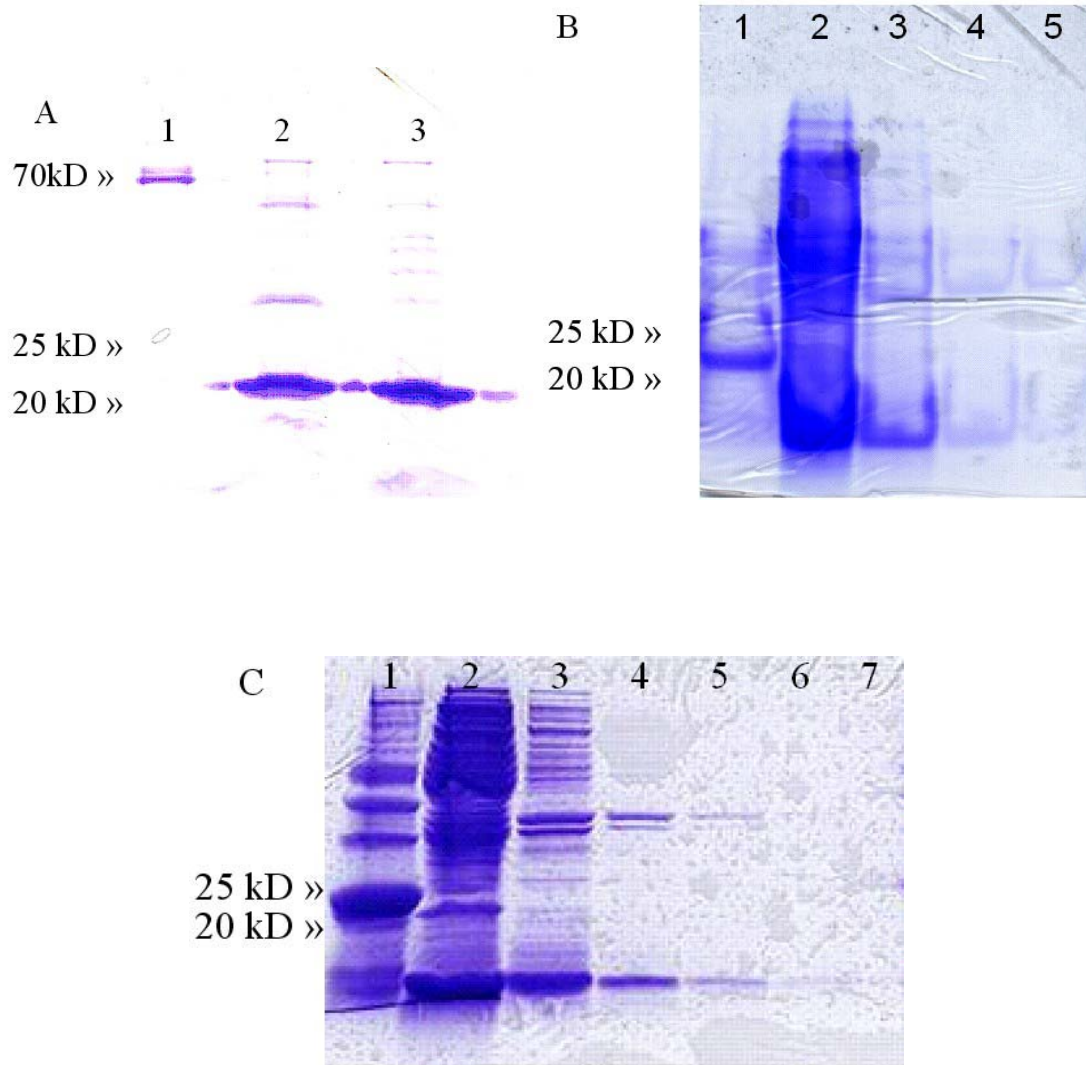


Figure 16. A, inclusion bodies expressed at 1.0 OD 600nm for 8 hours after inducing with 0.2% Arabinose and 1 mM IPTG in the BL21-AI pathway. Sonication steps included 90 second intervals of sonic treatment. Lane 2 is wild type sCD16A and Lane 3 is the sCD16A F176V mutant. B, sCD16A G147D mutant expressed with the same conditions as part A. Lane 1 is sCD16A G147D inclusion bodies, while Lanes 2 through 5 are the sonication supernatants in order. C, An example of a poor inclusion bodies sample. Lane 1 is the poor inclusion body sample and Lanes 2 through 7 are the sonication supernatants. All three gels were 12% Tris-Hcl (Bio-Rad) with 50  $\mu$ l wells. All samples were 25  $\mu$ l inclusion bodies and 25  $\mu$ l reducing buffer.

### 3.4 Refolding Results of sCD16 Protein

The refolding experiments proved to be very difficult and time consuming. At first the treated inclusion bodies were refolded by a stepwise dialysis method where the inclusion bodies were dissolved in an 8.5 M Urea solution and slowly dialyzed against a refolding buffer with a lower concentration of Urea each round (8.5, 6, 4, 2, 1, 0.5 M) until there was 0 M Urea [1]. At this point the proteins would be completely refolded and its buffer exchanged to an appropriate storage buffer. This process failed at the level of 0.5 M Urea every time due to heavy precipitation [1]. Steinle and Li, et al., acknowledged that precipitation may occur after all protein has been dissolved and that they will be misfolded aggregates [1]. The experiment produces yields in the 2- 5% range, on average. However, the precipitation occurred while refolding agents were still present and protein analysis showed minimal amounts of sCD16 in the solution. The process took several weeks to complete, so after many failed attempts a new process was sought out.

Another refolding process that was attempted was to create a gradient refolding buffer that pushed the dissolved inclusion bodies through a size exclusion column made of Sephadex G- 50 packed beads [63, 64]. The inclusion bodies were loaded into the column and pushed through in the presence of a refolding buffer whose gradient went from 8.5 M Urea to 0 M Urea. The beads would separate the proteins based on size and the gradient would refold the proteins. Two sizes of Sephadex were tried, G-50 and G-200. The fractions collected showed that the sizes of the beads were incorrect as one size didn't separate the proteins (Figure 17) and the other size blocked the proteins from entering the bed. Functional characterization showed that the proteins were not totally refolded properly. Lastly, the amount of inclusion bodies put into the column was far too insufficient to obtain the necessary concentration level of 10 mg/ml (Figure 17).

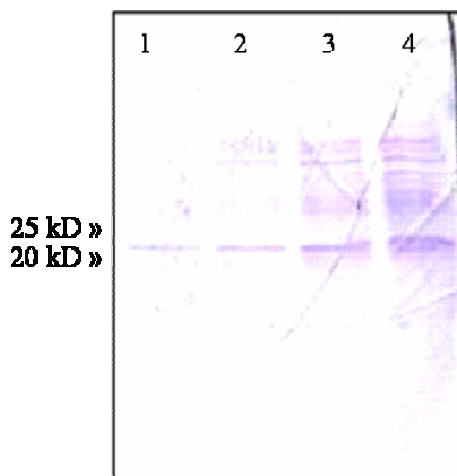


Figure 17. SDS-PAGE of refolded sCD16A wild type fractions from G-200 Sephadex size exclusion column with a Urea gradient. Proteins were not separated well enough and are far too low in concentration to make a final refolded sCD16 solution of 10 mg/ml. A Bio-Rad 12% Tris-HCl polyacrylamide gel was used with 25µl sample.

The third process was a Rapid Dilution Injection method [3]. Two injections of 50 mg of inclusion bodies each are added to 1 L of stirring refolding buffer (.4 M L-Arginine, .1 M Tris, 2 mM EDTA, 5 mM glutathione reduced, .5 mM glutathione oxidized, .2 mM PMSF, pH 8.0) over two days time. This process created the most controlled results and the best amount of properly refolded protein. Figure 18 shows a coomassie blue stain of stir cell refolded sCD16A after SDS-PAGE. The only variable in this process was the amount of solution the refolded buffer resides in. The entire amount needed to be concentrated down to create a 10 mg/ml concentration. Functional testing ensured that the protein was refolded properly. Also, optimal concentration occurred when concentration immediately followed the refolding process without any delay. A very low amount of aggregation would sometimes occur after the first day of refolding. This aggregation would be physically removed with a syringe before injecting the solution for a second time. The refolding solution continued to stir at 4° C while the stir cell concentrated the first 300 ml of solution.

### 3.5 Concentration of Refolded sCD16

After choosing to continue with the Rapid Dilution Injections [3] to refold the sCD16 proteins, concentration methods were attempted that allowed the sCD16 proteins to reach a minimum of 10 mg/ml without causing precipitation. It was also beneficial if the proteins can be washed to rid the solution of unwanted cellular proteins that may have been present in the inclusion bodies. A dialysis bag method [1, 62] was used at first in which the refolded proteins in refolding buffer were put in SnakeSkin (Pierce) dialysis bags with a molecular weight cutoff of 10 kD and covered with polyvinylpyrrolidone. This method concentrated 1 liter of buffer within 24 hours under very careful visual supervision as polyvinylpyrrolidone levels needed to be maintained. However, the powder caused the dialysis bags to dry out and stiffen, if allowed to continue for too long, and target protein recovery from the bags was often difficult. Careful washing of the inside of the tubing occurred with little protein recovery. SDS-PAGE would show only the slightest trace of refolded protein. In attempt to concentrate the solution to 10 mg/ml, the bags ended up too flat and eventually dried out. Typical concentration was about 30 to 1 ratio of pre-volume to post volume.

A second method entailed using a Centricon Plus-70 Concentrator tube with high volume capacity [65]. 70 ml could be concentrated per container with the Beckman rotor holding four centrifuge containers at once. The Centricon tubes yielded an increased concentration of 50 to 1. The containers would still have to be used multiple times, which caused precipitation of the proteins in the concentrator filter's membrane. This damaged the membrane's functioning ability and the ability to effectively use this method. Centrifugal filter devices were still not an ideal solution due to protein damage from having a low volume capacity and a large volume needing to be concentrated.

Using a 350 ml Amicon stir cell from Millipore was the eventual solution [4, 5]. The entire 1 liter of solution could be concentrated in 3- 7 days. The Amicon stir cell used a 10 kD NMWL Ultracel Amicon UltrafiltrationDisc membrane (Millipore) and a

nitrogen gas tank that pushed the stirring solution through this membrane. Figure 18 shows SDS-PAGE analysis (Pierce 12% Tris gel, 50  $\mu$ l well, 25  $\mu$ l sample) of target protein and the increased concentration and purity after using a stir cell. Figure 18A contains SDS-PAGE samples of wild type sCD16A and sCD16A F176V from the initial concentrations by a stir cell and by subsequent concentrations by iCON concentrators. Figure 18B shows the same thing only with sCD16A G147D. The effectiveness of the dual concentration is quite clear.

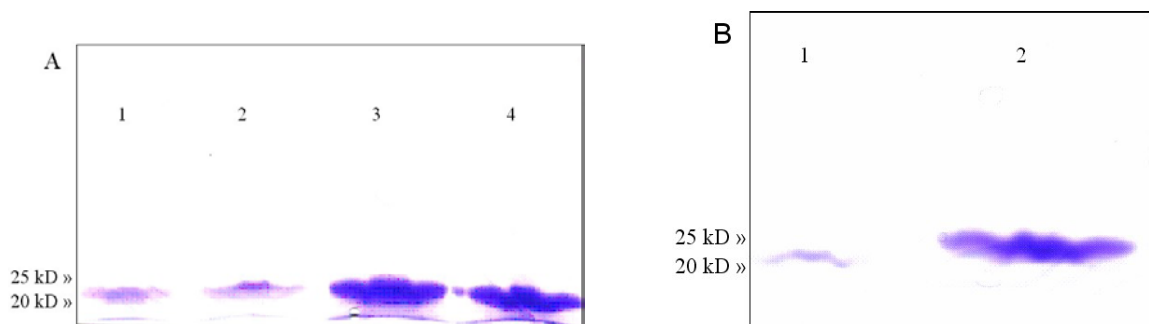


Figure 18. A, SDS-PAGE analysis on refolded sCD16 proteins. Lane 1 is refolded wild type sCD16A protein and Lane 2 is refolded sCD16A F176V mutant protein. Both samples taken from the post stir cell concentration solution. Lanes 3 and 4 are the same wild type and mutant protein after a second concentration in Pierce iCON concentrators. B, The same process as A, only with refolded sCD16A G147D mutant.

The other positives of using the stir cell to concentrate the solution were a lack of precipitation, the removal of most of the unwanted, excess proteins, and the ability to wash the proteins in the eventual storage buffer, 10 mM Tris. The refolding buffer was concentrated to a level between 20-50 ml. It was very rare for any aggregation to occur and physical removal by way of a syringe would rid this precipitation so that the membrane would not become clogged. A series of washings in 10 mM Tris occurred upon completion of concentration. A final volume between 20-40 ml was taken out of the stir cell with careful washing of the membrane itself to collect any proteins residing on its surface. Additional concentration experiments took place in 15 ml Falcon tubes

with Pierce 7ml iCON Concentrator membranes [60]. Figure 18, above, shows a second concentration of the refolded protein to approximately 10 mg/ml. The second concentration allowed for fine tuning of the concentration after Micro BCA (Pierce) protein estimation so that a level of 10 mg/ml was reached [61]. It also allowed for further washing of the solution. In most occurrences the protein purity was well above 90-95% and crystal trials began soon after, as long as functional characteristics were within range [44].

In the case of purity, a coomassie blue stain and silver stain were needed to verify that the protein solution was clean (greater than 90-95%) [54]. However, SDS-PAGE with a protein in Tris buffer could show results that looked like trace proteins in a silver stain [54]. Affinity chromatography with CLB coated Sepharose (GE Healthcare) beads [4, 5, 54] or an automated S-300 size exclusion column (Bio-Rad) were attempted in order to purify sCD16 proteins. However, every attempt made to use the affinity column ended with a clogged pre-column (plain Sepharose beads). The automated column had 8 ml fractions, which were too large for this process. A large peak on the OD readout was present at the correct location for sCD16 and SDS-PAGE analysis showed this fraction in Figure 19. The fraction did not provide a clean enough sample and was low in concentration due to the limit of a 2.5 ml injection of protein, which was not allowed to be made of high concentration for fear of clogging the column. This problem was never resolved but the majority of refolded proteins were already pure enough to warrant crystal trials.



Figure 19. SDS-PAGE of S-300 fraction contained sCD16A wild type.

The storage buffer of the refolded protein also played an important role. Soluble protein exhibited precipitation in certain buffers and temperatures [45]. At first protein was stored in 1x sterile PBS buffer. There was no precipitation in this buffer, but it was not an ideal buffer for growing crystals [45]. A second buffer, sterile Tris buffer, was better suited for making crystals but showed precipitation with certain environment changes. If kept at 4° C for too long, some protein would precipitate and drop the concentration below the target 10 mg/ml. Also, during crystal trials, the protein was reported to be sensitive to sudden thawing. Two Tris buffers were tested, 100 mM and 10 mM. The protein seemed to be more stable with the 10 mM and crystals grew better when in the 10 mM Tris buffer. Care has been taken to store the refolded solution at several temperatures, -70° C, -20° C, and 4° C, to record which gave the best results. As crystals can take months to grow, results will not be available for some time.

### 3.6 Functional Testing of sCD16 Proteins

After the refolding process, care was taken to ensure that sCD16 proteins were refolded correctly by testing the protein functioning ability. Recent experiments by Dr. Selvaraj's laboratory and Dr. Zhu's has established binding properties of CD16A and the

site specific mutants expressed in a eukaryotic pathway (Figure 21). Sandwich ELISA (Enzyme- linked Immunosorbant Assay) studies were carried out on wild type sCD16A and two mutants, sCD16A F176V and sCD16A G147D (Figure 20). These proteins were coated onto ELISA plates overnight, blocked with ELISA buffer (1x PBS, 1 mM EDTA, 1% FCS, 0.5% Tween), bound with Immune Complex, bound with 2<sup>ry</sup> antibody (Goat-anti-mouse-HRP), and developed with Amersham TMB Developer (GE Healthcare). Plates were read at 415 nm in an ELISA reader (Bio-Rad) and compared to positive control (CD16A-Ig) and negative control. The ELISA results were comparable to separate studies performed in Dr. Selvaraj's lab dealing with the same CD16 mutants expressed in a eukaryotic pathway, which indicated that these three proteins have refolded properly. According to the purity, functional data, and the concentration, crystals could now be made for the wild type sCD16A and the two site specific sCD16A mutants (F176V and G147D).

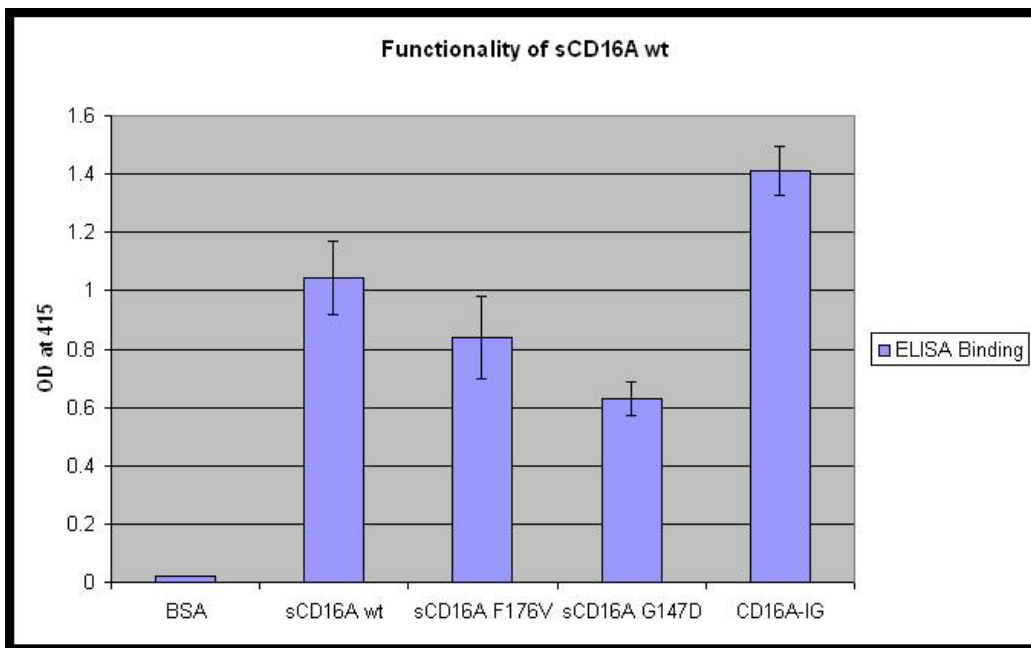


Figure 20. Results of Sandwich ELISA. See text for explanation of experiment. CD16A-Ig was used as a positive control, while BSA solution served as a negative control.

## CHAPTER 4

### DISCUSSION

#### 4.1 Current status and errors in the creation of sCD16 gene and sequencing

Three soluble CD16 proteins (sCD16A wild type, sCD16A F176V, and sCD16A G147D) were expressed to an optimal level, refolded properly, and were of sufficient purity to have begun crystal trials. These trials are currently ongoing as crystals have been growing and data is being collected. The mutant sCD16B proteins have not been expressed and refolded to the appropriate level for several reasons. Two of the proteins (sCD16B<sup>NA1</sup> D147G and sCD16B<sup>NA1</sup> V176F) never made it through the sequencing analysis after introducing the extracellular gene into the new pET 21a+ vector.

The extracellular portions of wild type CD16A and CD16B are approximately 97% identical and the wild type<sup>NA1</sup> and<sup>NA2</sup> alleles of CD16B are 95% homologous [24]. Therefore, it is an unknown reason as to why the sCD16B<sup>NA1</sup> mutants had incorrect sequences compared to the other mutants, even after several repetitions of the extracellular gene construction. Sequencing experiments were conducted by two different labs and analyzed using DNA sequencing software (Jellyfish). Sondermann, et al. [4], and Zhang, et al. [5], were able to obtain the extracellular portion of CD16B through similar steps in each of their experiments and the extracellular sequence cutoff of the gene was very similar to the previous studies, although the vectors were slightly different. Possible reasons for the poor sequencing were errors in the PCR experiment, including the primers binding to incorrect areas and high temperature heating causing adverse effects, and the digestion of more than just the ends of the gene before ligation. However, due to the extreme similarity between CD16B<sup>NA1</sup> and CD16B<sup>NA2</sup>, this is highly

unlikely. One other issue with the creation of the extracellular portion of the gene was the lack of a His- tag [67, 70]. An attempt to insert this sequence was thwarted by the creation of an unwanted restriction enzyme site which interfered in the process of ligating the gene into our chosen vector. The restriction sites needed for the His-tag would digest the CD16 gene in multiple locations and, therefore, could not be used.

The last two proteins (sCD16B<sup>NA2</sup> V176F and sCD16B<sup>NA2</sup> D147G) never expressed to a high enough level during induction experiments [4, 5] despite showing correct sequencing. Induction experiments were conducted using both the BL-21 AI pathway (Invitrogen) [49] and the BL-21 RIPL pathway (Stratagene) [59] to no avail. Neither showed any protein with the AI pathway after being expressed dozens of times with various durations (Figure 15) and starting Optical Densities (600 nm). The second pathway produced very minimal results with sCD16B<sup>NA2</sup> V176F when induced for 12 hours starting at an OD 600 nm value of 1.0. However, the protein was no more than 15% of the total Inclusion Bodies and the expression hasn't been reproduced. Refolding experiments could not take place from these results as the yield would be extremely low and the sample would be far too impure [1, 2, 4, 5, 70]. Expressing quality inclusion bodies made primarily of the target protein has proven to be a difficult process [1, 2, 44, 67, 70]. Usually, changing the starting conditions or the expression pathway will resolve the issue [1, 2, 44]. Mutations in the protein could make it more susceptible to bacterial processes that are not present in human cells that can result in degradation [44, 70]. This can be especially so with expression durations lasting more than 12 hours, which would already be harmful for normal proteins due to degradation.

#### **4.2 Functional Testing of the soluble sCD16 Protein**

A separate study in Dr. Selvaraj's lab, conducted by Ravichondran has shown that all six mutants involved in this study have been expressed in CHO-K1 cells and yielded active proteins. Figures 21 and 22 show these results. This experiment was conducted

by transfecting CHO-K1 cells with a mammalian expression vector, which contained the mutant CD16 genes, selecting cells by panning and then analyzing the expression by using flow cytometry. The experiments suggested that the CD16 mutants had various levels of avidity for the immune complex but were all unable to bind to monomeric IgG. The wild type sCD16A and the two sCD16A site specific mutant (F176V, G147D) proteins that have been expressed showed functioning characteristics in the Sandwich ELISA binding studies comparable to the results put forth by this study. Although not a bacterial expression pathway, it still shows that all the mutants can be expressed in an active state in a eukaryotic pathway. This, along with Sondermann et al. [4] and Zhang et al. [5] success, show that further changes in the expression pathway, and more specifically a change in the vector, should give better results for all the sCD16B mutants.

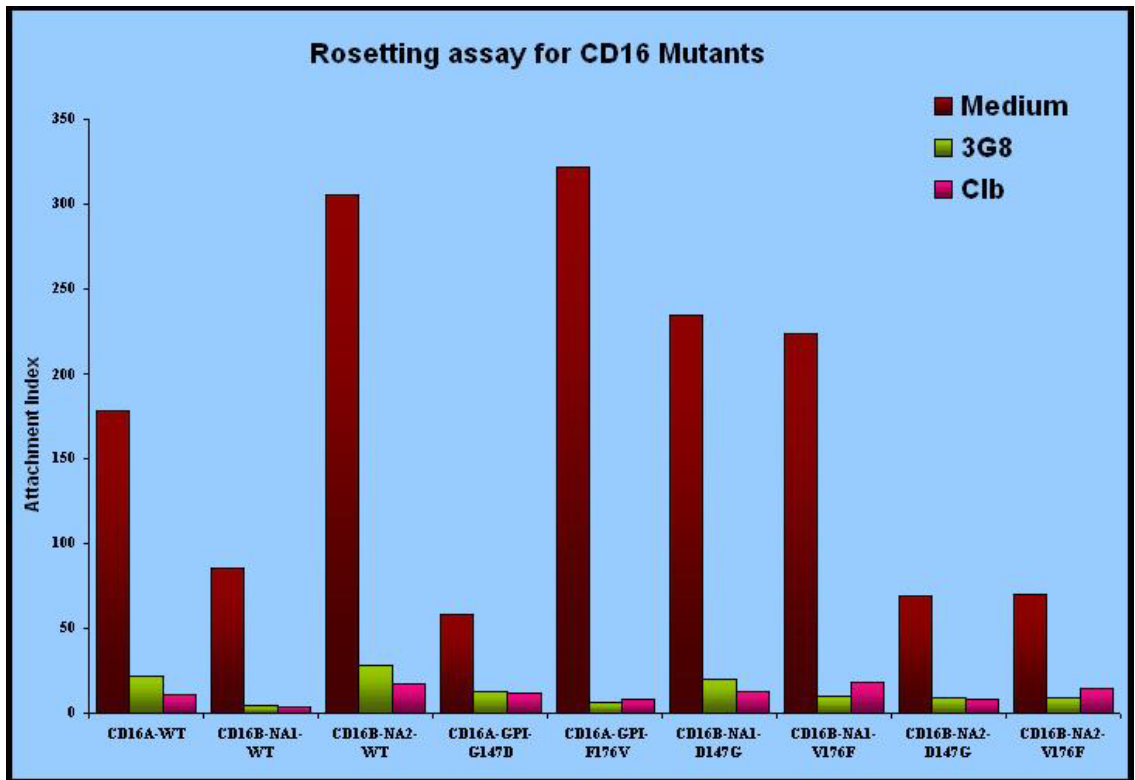


Figure 21. Rosetting assay for CD16 Mutants. Rosetting results (Figure 19) show binding activity of wild type CD16A and the six site specific CD16 mutants expressed in a eukaryotic pathway. Experiment performed by Ravichandran Panchanathan.

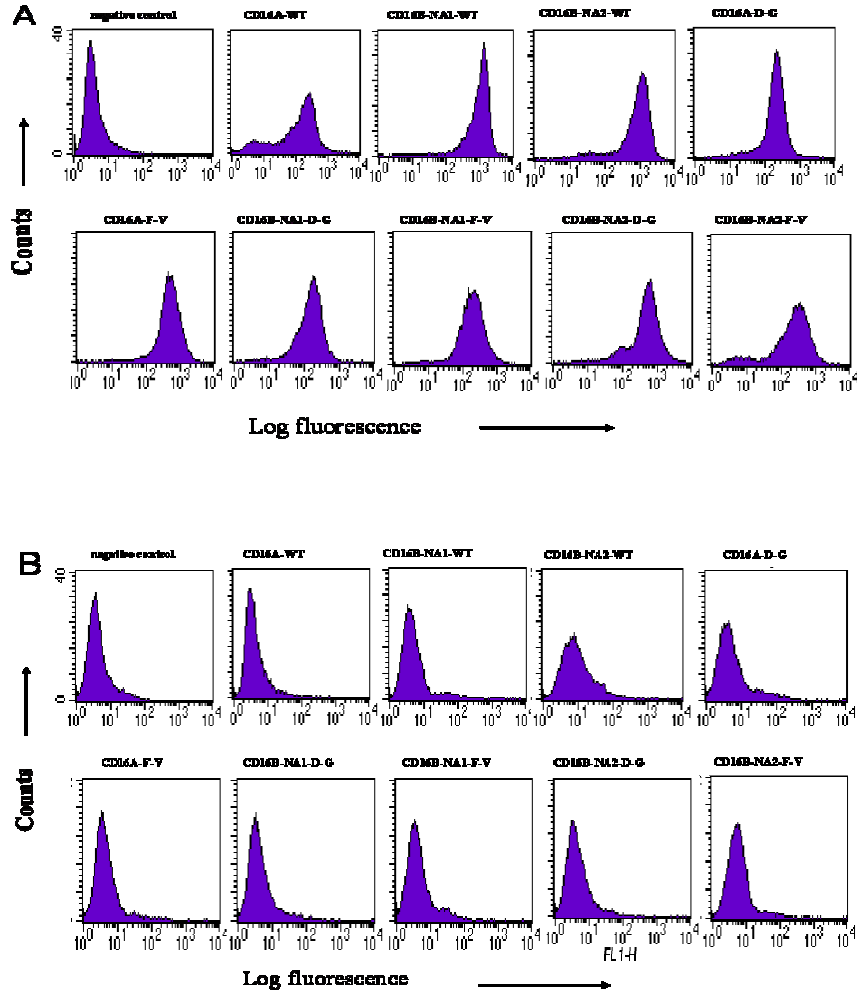


Figure 22. Rosetting results for Figure 18. A, Results show expression of CD16 mutants on CHO-K1 cells. B, Results show CD16A does not bind to monomeric IgG.

### 4.3 Expression of sCD16

The wild type sCD16A and the two sCD16A mutants (F176V and G147D) expressed very well (Figure 16) in the BL-21 AI pathway provided by Invitrogen [49]. This pathway was designed specifically for pET vectors (Novagen) and utilized L-Arabinose to aid IPTG in turning on the transcription mechanism. The vector, pET 21a+, was under the control of the Lac operon and used IPTG to release the repressor of transcription to allow for production of the protein (Figure 14B). The AI pathway

involved a second control point, the araBAD promoter, which tightly regulated expression in this particular vector [49]. L- Arabinose turned this promoter on allowing for IPTG to induce the target protein. Ideal conditions for the expression of the sCD16A proteins included growing seed cells for 16 hours at 32° C prior to induction [54]. Next, the protein was induced by adding 0.2% L-Arabinose and 1 mM IPTG at 1.0 OD at 600nm and continued incubation for 7 to 10 hours. Standard induction began at 0.4 OD at 600 nm and would continue for approximately 6 hours [1]. This induced the protein when cell growth reached the log phase and continued for a duration of time long enough to accumulate protein but short enough to prevent proteolytic degradation [45]. However, this did not produce the best yield of the target protein in the inclusion bodies. Better yields were typically found with a slightly higher starting cell concentration due to the higher number of cells initially producing the target protein [1, 2].

Optimal induction times tended to vary depending on the efficiency of the pathway, the protease buildup, and the production of other cellular proteins [1, 45]. In our case, the target protein was produced at six hours induction time but didn't develop optimal inclusion bodies until 8-10 hours (Figure 14A). Optimal inclusion bodies were made up of a very high percentage of target protein, which in turn gave the best refolding results [1, 2]. The use of the second pathway, BL-21 RIPL (Stratagene), was to supply the expression environment with extra amino acids that may be in demand in a bacterial expression pathway, limiting the quality of the inclusion bodies produced [45]. The second pathway produced worse results than the Invitrogen pathway in all three sCD16A proteins (wild type, F176V and G147D mutants). It is possible that the second control point in the AI pathway was able to tightly regulate all cellular proteins until the L- Arabinose was added, providing a higher yield of target proteins. Also, the second pathway, RIPL, may have increased target protein toxicity [45].

#### 4.4 Refolding of sCD16 From Dissolved Inclusion Bodies

After the optimal inclusion bodies were obtained, refolding experiments were performed. Several methods of refolding were used with varying effectiveness [67, 70]. The first method involved using Pierce SnakeSkin [1, 62] dialysis tubing to bring the Urea out of the dissolved inclusion bodies very slowly and thus forcing the protein to refold in a steady fashion. This slow process ideally produces a higher yield of refolded target protein by keeping total control of the process while at the same time keeping the volume low [1, 2, 45, 70]. However, there was significant precipitation as the solution crept closer to 0 M Urea. When using the step down method, there is usually a critical refolding point and if it is not reached, or if the process occurs too quickly, the proteins will form aggregates or turn into inclusion bodies again and precipitate due to the low amount of Urea [1]. This refolding point is different for every protein. Also, the amount of refolding buffer used to dilute the Urea and drive the folding was 5 liters. According to refolding protocols [1, 2, 3, 45, 70], a larger amount of solution was recommended as the additives in the refolding solution have a great effect on the dissolved proteins [46] and with a high starting concentration of those proteins, a greater amount of refolding buffer could only help. However, this increases the scale of the experiment to a much larger size. Using this refolding method was very time consuming and with continued precipitation, we felt we would get better results using smaller portions of the dissolved inclusion bodies and forcing the protein to refold quickly [2, 3].

A second refolding method involved a size exclusion Sephadex column and a Urea gradient, which forced refolding, separated the proteins, and removed the Urea [70]. This process is becoming more popular but is still tough to accomplish [70]. The size of the Sephadex beads needed to be changed to G-75 or G100 to allow the target protein to pass through the column while blocking out larger proteins. Even if these changes would

work, it would still not provide the necessary final concentration as the scale would be too small [4, 5]. Figure 17 shows some of the eluted fractions from the column.

The refolding method that produced the best results was the rapid dilution method [2, 3, 45]. These results showed that the refolded sCD16 proteins (wild type and mutants F176V, G147D) exhibited similar binding to the previously mentioned study from our lab (Ravichondran). This confirmed the active state of a correctly refolded protein. After concentrating to 10 mg/ml using an Amicon stir cell (Millipore), the protein purity was checked by SDS-PAGE and shown to be greater than 95% purity in the gels (Figure 13). This was adequate enough to start producing crystals from wild type sCD16A, sCD16A F176V, and sCD16A G147D. Some samples showed residual proteins upon concentration. Washing the solution several times and readjusting the concentration usually rid the solution of most of these unwanted trace proteins as they passed through the filter or precipitated in the filter and were discarded after centrifugation (Figure 23). Some target protein was also lost in this process, which called for a readjustment in concentration. In the instance that washing did not work, the sample was discarded. All affinity column purifications attempted, including CLB affinity chromatography, failed to produce any positive results as the protein never make it through the column. The lack of a His-tag was the most likely cause of this problem [47]. Several types and sizes of columns were used but none produced adequate results. Although there was no chromatography purification, crystal trials still produced excellent results due to a high concentration of pure protein shown by the SDS-PAGE on the wild type sCD16A and the two mutant sCD16A proteins (F176V and G147D), shown in Figure 18.

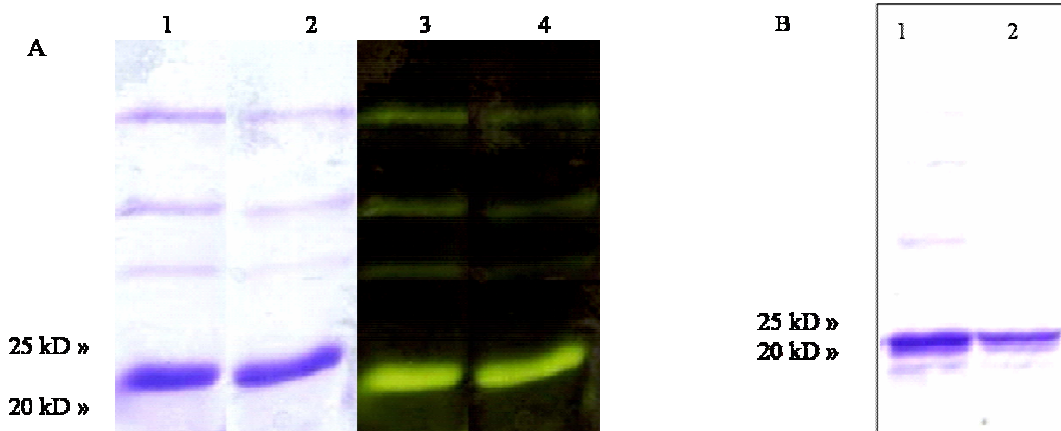


Figure 23. SDS-PAGE washing results of refolded wild type sCD16A. A, One washing step with 10 mM Tris buffer to help rid solution of unwanted protein. Lanes 1 and 3 are the same (pre-washing), as are Lanes 2 and 4 (post washing). Lanes 3 and 4 are the negative representation to aid in viewing the bands. B, A second example of washing to rid solution of trace proteins.

#### 4.5 Future Work and Conclusions

Recommended future work after the expression and refolding of the three sCD16A proteins (wild type, F176V, and G147D) includes several experiments. First, the continuation of the crystal trials for the three proteins already expressed and refolded. Current efforts by Dr. Zhu's lab (Wei Chen and Chris Curry) include using diffraction data received from sCD16A F176V crystals to solve the sCD16A F176V structure using molecular replacement with sCD16B<sup>NA2</sup> as a search model. Crystals have grown in four different conditions. The first was 0.1 M Citric Acid (pH 3.5) and 2.0 M Ammonium Sulfate. The second was 0.1 M HEPES (pH 7.5) and 1.4 M tri-Sodium Citrate Dihydrate. The third was 3.5 M Sodium Formate (pH 7.0). And fourth was 60% v/v Tacsimate (pH 7.0). Four optimized conditions, all at room temperature, produced diffraction data. The first was 2.2 M Ammonium Sulfate and 0.1 M Citric Acid (pH 2.5). The second was 3.1 M Sodium Formate (pH 6.5). The third and fourth were 3.9 and 3.7 M Sodium Formate (pH 7.0). The crystals were diffracted by Annie Heroux at the National Synchrotron

Light Source to a 1.6 Å resolution. Ongoing efforts also include growing crystals for wild type sCD16A and the sCD16A G147D mutant.

The expression of sCD16B<sup>NA1</sup> D147G, sCD16<sup>NA1</sup> V176F, sCD16B<sup>NA2</sup> D147G, and sCD16B<sup>NA2</sup> V176F mutants should include a different vector. A different pET vector (pET 28) may be the best place to start since the BL21- AI conditions have been established. The inclusion of a His-tag is recommended, which would increase the effectiveness of affinity chromatography purification. It is also recommended that the same sonication, refolding, and concentration protocols be followed initially as they too have been established. Also of significance, are attempts at purifying target proteins while still in the dissolved inclusion bodies state before refolding [74]. This may be a method to speed up the current process of sCD16A proteins (wild type, F176V, and G147D) that are still lacking the His-tag sequence.

In conclusion, the study of the FcR family, and more specifically the FcR-Ig interaction, is of great significance to immunology and autoimmune disease research. Future drug designs to fight disease and the alleviation of specific allergic reactions need functional and structural data. CD16 structural data, obtained from the proteins expressed in this project, can be used to develop methods of altering its Ig interactions to help alleviate symptoms or to prevent them from starting. It also lends information to the entire FcR family to possibly develop a method that has an effect on all members due to the significant homology of the extracellular domains. With the continued improvement of crystallization technology, better structural models can be developed, which will aid in the understanding of FcR's. Improvements in soluble protein expression through prokaryotic pathways can make this process all the more effective. With time, the wild type sCD16A structure will be solved from this project. Then, matching the mutant data with the previously proposed models and the ongoing mechanical studies will give a more complete picture of the CD16 receptor and possibly lead to future breakthroughs autoimmune disease treatments.

## REFERENCES

- [1] Steinle A, Li P, Morris DL, Groh V, Lanier LL, Strong RK, Spies T: Interactions of human NKG2D with its ligands MICA, MICB, and homologs of the mouse RAE-1 protein family. *Immunogenetics* 2001; 53: 279-87.
- [2] Altman, J: PHS 398. Rev. 5/1995: 27-40.
- [3] Garboczi: Folding of MHC-1 Monomers. NIAID Tetramer Core Facility Protocols.
- [4] Sondermann P, Huber R, Oosthuizen V, Jacob U: The 3.2-Å crystal structure of the human IgG1 Fc Fragment-FcγRIII complex. *Nature* 2000; 406: 267- 273.
- [5] Zhang Y, Boesen CC, Radaev S, Brooks AG, Fidman W-H, Sautes-Fridman C, Sun PD: Crystal Structure of the Extracellular Domain of a Human FcγRIII. *Immunity* 2000; 13: 387-395.
- [6] Maxwell KF, Powell MS, Hulett MD, Barton PA, McKenzie IF, Garrett TP, Hogarth PM: Crystal structure of the human leukocyte Fc receptor, Fc gamma RIIa. *Nat Struct Biol* 1999; 6: 437-442.
- [7] Sondermann P, Huber R, Jacob U: Crystal structure of the soluble form of the human Fcγ-receptor IIb: a new member of the immunoglobulin superfamily at 1.7Å resolution. *EMBO Journal* 1999; 18: 1095-1103.
- [8] Selvaraj P, Nimita F, Nagarajan S, Cimino A, Wang G: Functional Regulation of Human Neutrophil Fc gamma Receptors. *Immunologic Research* 2004; 29: 1-11.
- [9] Kimberly RP, Wu J, Gibson AW, et al.: Diversity and duplicity: human Fc gamma receptors in host defense and autoimmunity. *Immunol Res* 2002; 26: 177-189.
- [10] Pritchard NR: B cell inhibitory receptors and autoimmunity. *Immunology* 2003; 108: 263-273.

- [11] Hogarth PM: Fc receptors are major mediators of antibody based inflammation in autoimmunity. *Curr Opin Immunol* 2002; 14: 798-202.
- [12] Salmon JE, Pricop L: Human receptors for immunoglobulin F: key elements in the pathogenesis of rheumatic disease. *Arthritis Rheum* 2001; 44:739-750.
- [13] Cohen-Solal J, Cassard L, Fidman WH, Sautes-Fridman C: Fc gamma receptors. *Immunology Letters* 2004; 92: 199-205.
- [14] Ravetch J, Bolland S: IgG Fc receptors. *Annu Rev Immunol* 2001; 19: 275-90.
- [15] Malavasi F, Tetta C, Funaro A, et al.: Fc receptor triggering induces expression of surface activation antigens and release of platelet-activating factor in large granular lymphocytes. *Proc Natl Acad Sci USA* 1986; 83: 2443-2447.
- [16] Sonderrmann P, Jacob U: Human Fc gamma Receptor IIb Expressed in *Escherichia coli* Reveals IgG Binding Capability. *Biol. Chem* 1999; 380: 717-721.
- [17] Brooks DG, Qui WQ, Luster AD, Ravetch JV: Structure and expression of human IgG FcRII(CD32). Functional heterogeneity is encoded by the alternatively spliced products of multiple genes. *J Exp Med* 1989; 170: 1369-1385.
- [18] Sonderrmann, P, Kaiser J, and Jacob U: Molecular Basis for Immune Complex Recognition: A Comparison of Fc- Receptor Structures. *J Mol Biol* 2001; 309: 737- 749.
- [19] Sorge NM, Pol WL, Winkel JGJ: Fc $\gamma$ R polymorphisms: Implications for function, disease susceptibility and immunotherapy. *Tissue Antigens* 2003; 61: 189-202.
- [20] Salmon JE, Millard SS, Brogle NL, Kimberly RP: Fc gamma receptor IIIb enhances Fc gamma receptor IIa function in an oxidant- dependent and allele sensitive manner. *J Clin Invest* 1995; 95: 2877-85.
- [21] Selvaraj P, Rosse WF, SilberR, Springer TA: The major Fc receptor in blood has a phosphatidylinositol anchor and is deficient in paroxysmal nocturnal hemoglobinuria. *Nature* 1988; 333: 565-567.

- [22] Galon J, Gauchet JF, Mazieres N, Spagnoli R, Storkus W, Lotze M, et al: Soluble Fc $\gamma$ R (Fc $\gamma$ RIII, CD16) triggers cell activation through interaction with complement receptors. *J Immunol* 1996; 157: 1184- 92.
- [23] Sautes C, Teillaud C, Mazieres N, Tartour E, Bouchard C, Galinha A, et al: Soluble Fc $\gamma$ R (sFc $\gamma$ R): detection in biological fluids and production of a murine recombinant sFc $\gamma$ R biologically active in vitro and in vivo. *Immunobiology* 1992; 185:207-21.
- [24] Nagarajan S, Chesla SE, Cobern L, Anderson P, Zhu C, Selvaraj P: Ligand binding and phagocytosis by CD16 (Fc gamma receptor III) isoforms. *J Biol Chem* 1995; 270: 25762-25770.
- [25] Kimberly RP, Ahlstrom JW, click ME, Edberg JC: The glycosyl phosphatidylinositol-linked Fc $\gamma$ RIII PMN mediates transmembrane signaling events distinct from Fc $\gamma$ RII. *J Exp Med* 1990; 171: 1239-1255.
- [26] Bolland S, Ravetch JV: Inhibitory pathways triggered by ITIM-containing receptors. *Adv Immunol* 1999; 72:149-177.
- [27] Unkeless, JC, Shen Z, Lin CW, DeBeus E: Function of human Fc gamma RIIA and Fc gamma RIIIB. *Semin Immunol* 1995; 7: 37-44.
- [28] Garman SC, Kinet JP, Jardetzky TS: Crystal structure of the human high-affinity IgE receptor. *Cell* 1998; 95: 951-961.
- [29] Maxwell KF, Powell MS, Hulett MD, Barton PA, McKenzie IF, Garrett TP, Hogarth PM: Crystal structure of the human leukocyte Fc receptor, Fc gamma RIIa. *Nat Struct Biol* 1999; 6: 437-442.
- [30] Sondermann P, Huber R, Jacob U. Crystal structure of the soluble form of the human fc gamma-receptor IIb: a new member of the immunoglobulin superfamily at 1.7 Å resolution. *EMBO J* 1999; 18: 1095-1103.
- [31] Anon. [www.bookrags.com/sciences/sciencehistory/x-ray-crystallography-woi.html](http://www.bookrags.com/sciences/sciencehistory/x-ray-crystallography-woi.html) (Accessed on Feb 22, 2006).

- [32] Anon. [http://www.biocrawler.com/encyclopedia/X-ray\\_crystallography](http://www.biocrawler.com/encyclopedia/X-ray_crystallography) (Accessed on Feb 22, 2006).
- [33] Garman SC, Wurzburg BA, Tarchevskaya SS, Kinet JP, Jardetzky TS: Structure of the Fc Fragment of human IgE bound to its high-affinity receptor FcεRIα. *Nature* 2000; 406: 259-266.
- [34] Sondermann P, Oosthuizen V: X-ray crystallographic studies of IgG-Fcγ receptor interactions. *Biochemical Society Transactions* 2002; 30: 481-486.
- [35] Kinet JP: The high-affinity IgE receptor (FcεRI): from physiology to pathology. *Annu Rev Immunol* 1999; 17: 931-972.
- [36] Letourneur O, Sechi S, Willette-Brown J, Robertson MW, Kinet JP: Glycosylation of human truncated FcεRI α-chain is necessary for efficient folding in the endoplasmic reticulum. *J. Biol. Chem* 1995; 270, 8249-8256.
- [37] Kanellopoulos JM, Liu TY, Poy G, Metzger H: Composition and subunit structure of the cell receptor for immunoglobulin E. *J Biol Chem* 1980; 255: 9060-9066.
- [38] Sayers I, et al: Amino acid residues that influence RceRI-mediated effector functions of human immunoglobulin E. *Biochemistry* 1998; 37: 16152-16164.
- [39] Powell MS, Barton PA, Emmanouilidis D, Wines BD, Neumann GM, Peitersz GA, Maxwell KF, Garrett TP, Hogarth PM: Biochemical analysis and crystallization of Fc gamma RIIa, the low affinity receptor for IgG. *Immunol Lett* 1999; 68: 17-23.
- [40] Hulett MD, Witort E, Brinkworth RI, McKenzie IF, Hogarth PM: Multiple regions of human Fc gamma RII (CD32) contribute to the binding of IgG. *J Biol Chem* 1995; 270: 21188-94.
- [41] Chothia C, Novotny J, Bruccoleri R, Karplus M: Domain association in immunoglobulin molecules. The packing of variable domains. *J Mol Biol* 1985; 186: 651-63.
- [42] Engelhardt W, Geerds C, Frey J: Distribution inducibility and biological function of the cloned and expressed human betaFc receptor II. *Eur J Immunol* 1990; 20: 1367-1377.

- [43] Li P, Selvaraj P, Zhu C: Analysis of competition binding between soluble and membrane-bound ligands for cell surface receptors. *Biophysical Journal* 1999; 77: 3394-3406.
- [44] O'Callaghan CA, Tormo J, Willcox BE, Blundell CD, Jakobsen BK, Stuart DI, et al: Production, crystallization, and preliminary x-ray analysis of the human MHC class Ib molecule HLA-E. *Protein Science* 1998; 7: 1264- 1266.
- [45] Anon. [http://www.embl.de/ExternalInfo/protein\\_unit/draft\\_frames/index.html](http://www.embl.de/ExternalInfo/protein_unit/draft_frames/index.html) (Accessed on March 16, 2006).
- [46] Umetsu M, Tsumoto K, Hara M, Ashish K, Goda S, Adschiri T, Kumagai I: How additives influence the refolding of immunoglobulin-folded proteins in a stepwise dialysis system. Spectroscopic evidence for highly efficient refolding of a single-chain Fv fragment. *J Biol Chem* 2003; 278: 8979-87.
- [47] Cabrita LD, Dai W, Bottomley SP: A family of E. coli expression vectors for laboratory scale and high throughput soluble protein production. *BMC Biotechnol* 2006; 6: 12.
- [48] Anon. <http://www.emdbiosciences.com/docs/docs/PROT/TB036.pdf> (Accessed on March 20, 2006).
- [49] Invitrogen: BL21-AI One Shot Chemically Competent Cells. Version B; October 7, 2002.
- [50] Sondermann P, Jacob U: Human Fcγ receptor IIb expressed in Escherichia coli reveals IgG binding capability. *Biol Chem* 1999; 380, 717-721.
- [51] Li P, Nagarajan S, Zhu C, Selvaraj P: Recombinant CD16-Ig forms a homodimer and cross-blocks the ligand binding functions of neutrophil and monocyte Fcγ receptors. *Mol Immunol* 2002; 38: 527-38.
- [52] Favre D: *Biotechniques* 1992; 13.
- [53] Qiagen: Qiaquick Gel Extraction Kit Protocol. *Qiaquick Spin Handbook* 2002; 7.

- [54] Sambrook J, Fritsch EF, Maniatis T: *Molecular Cloning, A Laboratory Manual*, Cold Spring Harbor Laboratory (NY), 2nd Edition, 1989; 1-3: 561-563.
- [55] Hanahan D: *J Mol Biol* 1983; 166: 557-580.
- [56] Invitrogen: BL21-AI One Shot Chemically Competent E. coli 2002; C6070-03.
- [57] Qiagen: QIAprep Spin Miniprep Kit 2005; Second Edition.
- [58] Invitrogen: One Shot TOP10 Competent Cells 2004; C4040-10.
- [59] Stratagene: BL21- CodonPlus (DE3) Competent Cells; 230240.
- [60] Pierce Biotechnology, Inc: Instructions for iCON Concentrator 7 ml/9K and 7 ml/20 K. 89884: 1516.0.
- [61] Pierce Biotechnology, Inc: Instructions for Micro BCA Protein Assay Kit. 23235: 0412.2.
- [62] Pierce Biotechnology, Inc: Instructions for SnakeSkin Pleated Dialysis Tubing. 68035: 0732.
- [63] Hagel L: *Gel Filtration in Protein Purification, Principles, High Resolution Methods and Applications*. Janon JC and Ryden L (editors). VCH Publishers Inc., New York 1989; 63-106.
- [64] Hagel L, Janson JC: *Size-exclusion chromatography*, in *Chromatography*, 5th edition. Elsevier, Amsterdam 1992; A267-AA307.
- [65] Millipore: Centricon Plus-70 Centrifugal Filter Device. Data Sheet. Pf460en00.
- [66] Qiagen: QIAprep Miniprep Handbook, 2nd Edition. November, 2005.

- [67] Pedelacq JD, Piltch E, Iong EC, Berendzen J, Kim CY, Rho BS, Park MS, Terwilliger TC, Waldo GS: Engineering soluble proteins for structural genomics. *Nature Biotechnology* 2002; 20: 927-932.
- [68] Sorge NM, van der Pol WL, van de Winkel JGJ: Fc $\gamma$ R polymorphisms: Implications for function, disease susceptibility and immunotherapy. *Tissue Antigens* 2003; 61: 189-202.
- [69] Wu J, Edberg JC, Redecha PB, Bansal V, Guyre PM, Coleman K, Salmon JE, Kimberly RP: A Novel Polymorphism of Fc $\gamma$ RIIIa (CD16) Alters Receptor Function and Predisposes to Autoimmune Disease. *J Clin Invest* 1997; 100: 1059-1070.
- [70] Li M, Su ZG, Janson JC: In vitro protein refolding by chromatographic procedures. *Protein Expression and Purification* 2004; 33: 1-10.
- [71] Chen J, Anderson JB, DeWeese-Scott C, Fedorova ND, Geer LY, He S, Hurwitz DI, Jackson JD, Jacobs AR, Lanczycki CJ, Liebert CA, Liu C, Madej T, Marchler-Bauer A, Marchler GH, Mazumder R, Nikolskaya AN, Rao BS, Panchenko AR, Shoemaker BA, Simonyan V, Song JS, Thiessen PA, Vasudevan S, Wang Y, Yamashita RA, Yin JJ, Bryant SH: MMDB: Entrez's 3D-structure database. *Nucleic Acids Res* 2003; 31: 474-7.
- [72] Kraulis PJ: MOLSCRIPT: a program to produce both detailed and schematic plots of protein structures. *J Appl Crystallogr* 1991; 24: 946-950.
- [73] Barton GC: ALSRIPT: tool to format multiple sequence alignments. *Protein Eng* 1993; 6: 37-40.
- [74] Gu Z, Weidenhaupt M, Ivanova N, Pavlov M, Xu B, Su ZG, Janson JC: Chromatographic methods for the isolation of, and refolding of proteins from, *Escherichia coli* inclusion bodies. *Protein Expr Purif* 2002; 25: 174-9.
- [75] Nimmerjahn F, Bruhns P, Horluchl K, and Ravetch JV: Fc $\gamma$ RIV: A Novel FcR with Distinct IgG Subclass Specificity. *Immunity* 2005; 23: 41-51.
- [76] Tschesche H: *Modern Methods in Protein- and Nucleic Acid Research*. Walter de Gruyter 1990; Berlin, New York.

- [77] Sundstrom M, Norin M, Edwards A: Structural Genomics and High Throughput Structural Biology. Taylor and Francis 2006; New York.
- [78] McRee D: Practical Protein Crystallography, 2<sup>nd</sup> Edition. Academic Press 1999; San Diego.
- [79] Rupp B. <http://www.ruppweb.org/Xray/101index.html> (Accessed on May 2<sup>nd</sup>, 2006).